Atmosphere-biosphere trace gas exchanges simulated with a single-column model

L. N. Ganzeveld and J. Lelieveld
Max-Planck Institute for Chemistry, Mainz, Germany

F. J. Dentener
Joint Research Center, Institute for Environment and Sustainability, Ispra, Italy

M. C. Krol and G.-J. Roelofs
Institute for Marine and Atmospheric Research Utrecht, Utrecht University, Utrecht, Netherlands

Received 27 March 2001; revised 17 December 2001; accepted 21 December 2001; published 27 August 2002.

[1] The exchange of oxidized nitrogen species (NO_x) between the biosphere and atmosphere is controlled by complex interactions between emissions, dry deposition, (photochemical) chemical transformations, and turbulent exchanges, all varying with height within the canopy. We have developed a multilayer atmosphere-biosphere trace gas exchange model to study the role of canopy interactions in the net atmosphere-biosphere NO_x exchange flux on a global scale. We evaluate this model, implemented in a single-column chemistry and meteorological model, for a selection of ecosystems by comparison with observations. The modeled and observed ozone and oxidized nitrogen concentrations and fluxes are generally in reasonable agreement if we constrain our model with site-specific surface and meteorological parameters. The sensitivity of atmosphere-biosphere trace gas exchange to nocturnal turbulent exchange appears to be large. A comparison of the NO_x fluxes calculated by the traditional big leaf approach and the atmosphere-biosphere model is presented. For sites that are exposed to relatively large anthropogenic emission fluxes, the big-leaf approach and biosphere model calculate similar NO_x fluxes, which confirms the applicability of the big-leaf approach for polluted regions. However, for relatively pristine sites, differences between the NO_x fluxes of the biosphere model and the big leaf approach are significant. This underscores the importance of an explicit representation of the biosphere processes for those locations where the NO soil emissions flux is comparable to or exceeds the anthropogenic emissions. *INDEX TERMS:* 0315 Atmospheric Composition and Structure: Biosphere/atmosphere interactions; 1615 Global Change: Biogeochemical processes (4805); 3322 Meteorology and Atmospheric Dynamics: Land/atmosphere interactions; 3379 Meteorology and Atmospheric Dynamics: Turbulence; *KEYWORDS:* Atmosphere-biosphere trace gas exchanges, micrometeorology, dry deposition, biogenic emissions, turbulence, canopy reduction factor

1. Introduction

[2] Recent studies of dry deposition processes of trace gases and aerosols, as incorporated in a chemistry and General Circulation Model (GCM), have shown the sensitivity of calculated concentrations and fluxes to the representation of these processes on a global scale [*Ganzeveld and Lelieveld*, 1995; *Ganzeveld et al.*, 1998]. The dry deposition flux is calculated from the surface layer concentrations and the dry deposition velocity, which reflects the turbulent transport to Earth's surface, molecular diffusion through the quasi-laminar boundary layer, and the surface absorption efficiency. Vegetation uptake of trace gases such as ozone (O_3) and sulfur dioxide (SO_2) is largely controlled by plant physiological processes and the canopy structure. The dry deposition velocity over vegetated surfaces is calculated in the coupled chemistry-GCM ECHAM (European Centre model, Hamburg version) applying the "big leaf" approach [e.g., *Hicks et al.*, 1987]. Since this approach is based on a large number of observations of dry deposition velocities of trace gases such as ozone and sulfur dioxide, it is expected to yield realistic deposition velocities for these trace gases for many locations and different seasons. This is confirmed by the agreement between the calculated and observed O_3 and SO_2 dry deposition velocities [*Ganzeveld and Lelieveld*, 1995; *Ganzeveld et al.*, 1998].

[3] The dry deposition scheme has also been applied to calculate the dry deposition flux of nitric acid (HNO_3), nitrogen oxide (NO) and -dioxide (NO_2). However, for the latter two trace gases, as well as for other reactive trace

0148-0227/02/2001JD000684$09.00

gases with comparable short chemical lifetimes, it can be questioned if the big leaf approach is valid. For a trace gas with a typical chemical lifetime smaller than or comparable to the turbulent timescale, fast chemical transformations result in a flux divergence, which is not accounted for by applying the traditional aerodynamic resistance formulas for turbulent transport. Moreover, the atmosphere-biosphere exchange flux of NO and NO_2 at the canopy top is bidirectional, dependent on the surface layer concentrations and interactions between the controlling processes within the canopy, e.g., emissions, dry deposition, chemistry, and turbulence. NO emitted from the soil reacts with O_3, producing NO_2, which is removed by dry deposition. NO_2 also reacts with the oxidation products of the emitted hydrocarbons, e.g., isoprene, forming organic nitrates (e.g., peroxyacetylnitrate (PAN)), which can be removed locally by dry deposition or transported over large distances. The effectiveness of the internal cycling of NO_x (NO + NO_2) within the canopy further depends on radiation flux densities within the canopy and the turbulent exchange between the canopy and the atmosphere. The chemical conversion of reactive trace gases as a function of height within the canopy is associated with decreasing photodissociation rates through the interception of radiation. Moreover, the residence time of the trace gases within the chemical regime of the canopy strongly depends on the turbulent mixing.

[4] The flux divergence of reactive trace gases within the canopy has been addressed in previous studies using observations and model simulations [*Jacob and Wofsy*, 1990 (hereinafter refered to as JW90); *Gao et al.*, 1993; *Duyzer et al.*, 1995; *Joss and Graber*, 1996; *Walton et al.*, 1997]. The use of multilayer trace gas exchange models, constrained by observations, is common among these studies. We have developed an atmosphere-biosphere trace gas exchange model, which is similar to the multilayer trace gas exchange models, but which can be used to study the role of the biosphere interactions for trace gas exchanges on a global scale. We have implemented the biosphere model in a single-column version of ECHAM4 [*Roeckner et al.*, 1996], coupled to a nonmethane hydrocarbon chemistry scheme. This allows evaluation of the biosphere model by comparison of the calculated canopy top fluxes with observations. The atmosphere-biosphere trace gas exchange model considers the dry deposition process, biogenic emissions of oxidized nitrogen and hydrocarbons species and the extinction of radiation and turbulence within the canopy. However, the model must be applicable in global-scale studies, imposing rather strong constraints on the model structure. Hence, the process description is highly parameterized and a coarse vertical and temporal resolution is applied. Another important limitation is related to the applied micro-meteorological, biophysical and biogeochemical input parameters to the vegetation model. The aforementioned case specific studies generally used observed site-specific biophysical parameters, such as the leaf area index (LAI), or biogeochemical parameters, such as the soil biogenic NO flux, to constrain the models [JW90; *Walton et al.*, 1997]. However, this detailed information is not available for many ecosystems on a global scale, which implies that we must rely on the available information in global databases.

[5] The implementation of the atmosphere-biosphere trace gas exchange model in the Single-Column Model (hereafter referred to as SCM) is described in section 2. Numerical issues relevant to the application of atmosphere-biosphere models are discussed in section 3. In section 4 we evaluate the atmosphere-biosphere trace gas exchange model by comparison with observations, and show the differences between the NO_x fluxes calculated by the big leaf approach and the biosphere model, followed by a discussion in section 5 and conclusions in section 6. In an accompanying paper [*Ganzeveld et al.*, 2002] we present an assessment of the role of biosphere interactions for the effective emissions of NO_x on a global scale.

2. Atmosphere-Biosphere Trace Gas Exchanges in a SCM

[6] For the development and evaluation of the atmosphere-biosphere trace gas exchange model we apply a single-column version of the general circulation model ECHAM4 [*Roeckner et al.*, 1996], the latter being used for global-scale studies. Use of the SCM offers the opportunity to perform process studies, e.g., of the sensitivity to the spatial and temporal resolution, and the development of parameterizations with an optimal consistency for application in ECHAM. Moreover, specific surface cover characteristics such as soil moisture and canopy structure can be prescribed for a consistent evaluation of modeled and observed parameters. The horizontal grid resolution of a global-scale chemistry-GCM like ECHAM is typically 100 km or more, which implies that the surface characteristics of the model grid cells with a heterogeneous coverage can be very different from the specific site characteristics. A disadvantage of using an SCM is that it only explicitly calculates the processes occurring at a spatial scale smaller than the typical grid size of ECHAM. This implies that for sites where the concentrations are being controlled by large-scale (>ECHAM's grid resolution) advection, in addition to the short-term, local-scale processes, e.g., dry deposition and biogenic emissions, the SCM will underpredict the calculated concentrations of the relatively long-lived trace gases. For a typical surface layer wind speed of about 5 m s^{-1}, a model integration exceeding one day already needs to include the contribution of advection of trace gases such as O_3 and NO_x from source regions at a distance of about 450 km. The SCM considers the contribution of advection of pollutants from source regions within an ECHAM grid square using monthly average anthropogenic emissions. However, these may differ substantially from the local influence of anthropogenic emissions during the observations. In section 4, we present a method to consider the advection of trace gases from source regions for the model evaluation of the trace gas concentrations and fluxes calculated by the SCM.

[7] The chemistry scheme used in ECHAM [*Roelofs and Lelieveld*, 1995, 1997, 2000], including specific modifications required for the study of atmosphere-biosphere trace gas exchange, has also been implemented into the SCM. The chemistry scheme used in this study calculates the concentrations of CH_4, CO, NO_y (NO, NO_2, HNO_4, NO_3, N_2O_5, PAN, methylperoxyacetylnitrate (MPAN) and HNO_3), OH, O_3, nonmethane hydrocarbons including iso-

prene (C_5H_8), and a selection of the resulting hydrocarbon oxidation products such as formaldehyde (CH_2O), higher aldehydes and acetone (CH_3COCH_3). Anthropogenic and biogenic emissions of NO_x, CO, CH_4 and higher hydrocarbons, including acetone, are considered using monthly mean global emission fluxes. Dry deposition processes are described using the big leaf resistance approach [*Ganzeveld and Lelieveld*, 1995; *Ganzeveld et al.*, 1998]. With the implementation of the atmosphere-biosphere trace gas exchange model, the calculation of the dry deposition and biogenic emission fluxes for the vegetated areas has been modified as described in the next section.

[8] The SCM needs to be initialized with vertical profiles of temperature, moisture, wind speed, trace gas concentrations and surface boundary conditions, e.g., surface temperature, soil moisture and the surface cover characteristics. For the initialization of the physical and dynamical parameters we apply the vertical profiles and surface properties of the grid cell of the ECHAM model most closely resembling the location of the SCM. The trace gas concentrations are initialized using monthly mean vertical profiles of trace gas concentrations from a tracer transport model [*Houweling et al.*, 1998; *Lelieveld and Dentener*, 2000]. At the time of the development of the SCM, the corresponding calculated ECHAM concentrations where not yet available. In this study the model integrations with the SCM have been performed using the default ECHAM vertical coordinate system of 19 atmospheric levels, with 5 layers in the planetary boundary layer (on average), 9 in the free troposphere, and 5 in the stratosphere.

2.1. Atmosphere-Biosphere Trace Gas Exchange Model

[9] The concentration tendency in the surface layer (SL) is calculated from the tendencies over the vegetation, wet skin (ws), bare soil and snow/ice cover fractions $fr_{veg/ws/soil/snow/ice}$:

$$\left(\frac{dc}{dt}\right)_{SL} = fr_{veg}\left(\frac{\partial c}{\partial t}\right)_{veg} + fr_{ws}\left(\frac{\partial c}{\partial t}\right)_{ws} + fr_{soil}\left(\frac{\partial c}{\partial t}\right)_{soil} + fr_{snow/ice}\left(\frac{\partial c}{\partial t}\right)_{snow/ice} \quad (1)$$

The concentration tendency in the surface layer over the bare soil and snow/ice fraction is calculated according to

$$\left(\frac{\partial c}{\partial t}\right)_{soil/snow/ice} = \left(\frac{\partial c}{\partial t}\right)_{turb} + \left(\frac{\partial c}{\partial t}\right)_{emis} + \left(\frac{\partial c}{\partial t}\right)_{dep} + \left(\frac{\partial c}{\partial t}\right)_{chem} \quad (2)$$

which reflects the contribution by turbulent transport between the surface layer and the layer aloft, biogenic as well as anthropogenic emissions, dry deposition, and chemical transformations. Note that chemical convection is ignored here. Since the coupling with the biosphere is now explicitly calculated by the vegetation model, equation 2 for the surface layer over the vegetation and wet skin fraction, reduces to

$$\left(\frac{\partial c}{\partial t}\right)_{veg/ws} = \left(\frac{\partial c}{\partial t}\right)_{turb} + \left(\frac{\partial c}{\partial t}\right)_{chem} \quad (3)$$

with the turbulent tendency reflecting the change in the concentrations due the turbulent exchange between the surface layer and the layer aloft as well as the turbulent exchange between the surface layer and the canopy-top layer of the vegetation model. Concentration tendencies within the canopy due to the turbulent exchange, emissions, dry deposition and chemical transformations are calculated according to

$$\left(\frac{dc}{dt}\right)_{canopy} = \frac{\Delta F_{turb} + F_{emis} - F_{dep}}{\Delta z} + P_{chem} \quad (4)$$

with Δz being the thickness of the canopy layer. Note that this is the discrete formula as applied in the numerical scheme. The calculation of the biogenic emission flux, F_{emis}, the dry deposition flux, F_{dep}, and chemical production or destruction, P_{chem}, are discussed more extensively in the next section. The turbulent flux is calculated based on local closure theory:

$$F_{turb} = -K_H \frac{\partial c}{\partial z} \quad (5)$$

where K_H is eddy diffusivity for heat and $\partial c/\partial z$ is the concentration gradient between the reference height of the surface and canopy layers. The eddy diffusivity profile in the canopy is estimated by scaling the surface layer K_H with the calculated wind speed for each layer relative to the calculated surface layer wind speed. The wind speed profile within the canopy is represented by an exponential function so that the wind speed is a function of the canopy height and an attenuation coefficient dependent on the canopy characteristics [*Cionco*, 1978]. We recognize that this is a rather simple approach of representing the turbulent exchange of trace gases between the canopy and the surface layer. However, since we do no consider the transfer of momentum, heat and moisture within the canopy in this study, its significance for the turbulent exchange of trace gases, e.g., the occurrence of free-convection conditions within the canopy, cannot be considered explicitly. The role of the canopy transfer of momentum, heat and moisture for the trace gas exchanges is discussed more extensively in section 5.

2.1.1. Dry Deposition, Biogenic Emissions, and Photochemistry Within the Canopy

[10] The original formulation of the dry deposition calculations is described by *Ganzeveld and Lelieveld* [1995] and *Ganzeveld et al.* [1998]. The algorithm calculates the dry deposition flux F_{dep} from the surface layer concentration and the dry deposition velocity V_d. The latter is calculated from the aerodynamic and quasi-laminar boundary layer resistance and the stomatal resistance [*Sellers et al.*, 1986] and ocean water, bare soil, cuticle, mesophyll and wet surface resistances. The dry deposition scheme has originally been developed for O_3, NO, NO_2, HNO_3, SO_2 and SO_4^{2-} aerosol. Additional resistances of the trace gases of the hydrocarbon chemistry scheme, for which the dry deposition process is expected to be a significant sink, have been estimated using the approach by *Wesely* [1989]. Based on the Henry's law coefficient and an estimated reactivity constant, the different uptake resistances are calculated by

scaling these with the SO_2 uptake resistances for soluble nonreactive trace gases, and with O_3 for nonsoluble reactive trace gases. The dry deposition calculations have been modified for the atmosphere-biosphere model calculating a "vegetation" dry deposition velocity for each canopy layer as the reciprocal value of the vegetation resistance. This resistance is calculated from the stomatal, mesophyll, cuticle resistance, a leaf boundary layer resistance and the amount of biomass in each layer. The leaf boundary layer resistance, which represents the diffusion through a thin layer adjacent the leaf surface, is calculated from the wind speed profile according to *Meyers* [1987].

[11] The selected uptake resistances of the original big leaf dry deposition scheme result in a small dry deposition velocity of NO, and an NO_2 dry deposition velocity which is about 2/3 of the ozone dry deposition velocity over vegetation [*Ganzeveld and Lelieveld*, 1995]. In contrast to the ozone and sulfur dioxide dry deposition velocities, the NO and NO_2 big leaf deposition velocities do not only reflect a biological sink but also sources from chemical transformations and biogenic emissions within the canopy. The presence of NO_2 and NO sources due to chemical production and the biogenic emissions, respectively, results in a decrease of the NO and NO_2 dry deposition velocity compared to the ozone dry deposition velocity for the big leaf approach. However, since these processes are explicitly resolved in the biosphere model, a zero NO_2 mesophyll resistance is applied whereas we assume zero uptake of NO by the leaves, corresponding to an infinite mesophyll resistance.

[12] The soil biogenic NO emission flux is calculated according to *Yienger and Levy* [1995] (hereafter referred to as YL95), however, without applying their canopy reduction factor (see section 4.2). The emissions of isoprene by the vegetation are calculated according to *Guenther et al.* [1995]. For more details concerning the calculation of the biogenic emissions we refer to the accompanying paper [*Ganzeveld et al.*, 2002].

[13] As has been mentioned above, the extinction of radiation in the canopy due to the interception by biomass needs to be considered since it controls the photochemistry within the canopy. Moreover, the biogenic emissions of hydrocarbons strongly depend on the radiation regime within the canopy. The vertical profiles of radiation within the canopy are calculated according to *Norman* [1979] and *Weiss and Norman* [1985]. The algorithm calculates the profiles of the direct and diffusive irradiance in both the visible (photosynthetically active radiation (PAR)) and near infrared spectral region from the net solar radiation [*Weiss and Norman*, 1985], the canopy structure and soil albedo. These radiation profiles are used to estimate the photodissociation rates within the canopy from the above canopy PAR flux and the surface layer photodissociation rate. This approach implies that the spectral leaf transmission of the photodissociation rates (e.g., of NO_2 at $\lambda \leq 420$ nm) in our model is similar to that of PAR ($\lambda = 400-750$ nm).

2.1.2. Canopy Structure

[14] The atmosphere-biosphere trace gas exchange model is initialized by biogeophysical parameters, e.g., the leaf area index (LAI), canopy height, surface roughness and the vertical distribution of biomass expressed by the leaf area density profile, and biogeochemical parameters such as emission factors. Since a part of this study entails the evaluation of the model performance by comparison with observations, the model is initialized with the available site-specific canopy characteristics to ensure a realistic comparison. However, the required input parameters are often not available and therefore the biosphere characterization partly relies on the parameter values derived from the global-scale data sources that we apply to define the canopy structure in ECHAM. For more details concerning the surface cover characterization in ECHAM we refer to *Ganzeveld et al.* [2002].

3. Spatial and Temporal Resolution

3.1. Vertical Grid Spacing

[15] To determine the number of vertical layers that need to be distinguished within the canopy to resolve the effect of the biosphere interactions on the flux divergence, simulations with the SCM with 1, 2 and 10 equidistant layers have been performed for a tropical rain forest canopy. For more details concerning the defined canopy structure we refer to section 4.1. The maximum number of 10 layers is selected based on an analysis showing that there is no significant change in the modeled fluxes and concentrations when more layers are added. This maximum number of 10 canopy layers would be unpractical for a global model. However, the results can be used to develop parameterizations for a one or two-layer vegetation model. Model integrations have been performed for one day using a time step of 10 seconds, using initial within-canopy concentrations similar to the surface layer concentrations. The short time step is required to continuously adjust the SCM to the observational constraints. Later we will show that there is no principal need to apply such a short time step in the framework of the global ECHAM model [*Ganzeveld et al.*, 2002]. Figures 1a, 1b, 1c, and 1d show the modeled canopy top (30 m) fluxes of radon, ozone, isoprene and the NO_x over a 24-hour period for the three vertical resolutions. These four trace gases are selected based on their distinctly different chemical behavior and lifetime, and the location and magnitude of the sources and sinks within the canopy. Figure 1a shows the modeled diurnal cycle of the canopy top flux of radon, for which we assume a constant soil emission flux of 0.3 atoms cm^{-2} s^{-1} [*Trumbore et al.*, 1990]. At night radon accumulates within the canopy, which results in an early morning peak flux after the breakdown of the surface layer inversion. The three vertical resolutions yield similar diurnal cycles. However, in the 1-layer model version the sunrise peak flux is larger than in the 2- and 10-layer model because the 1-layer version does not account for turbulent transport between the soil and canopy crown. Note that the shown 24-hour average Rn canopy top flux ($\sim$0.26 atoms cm^{-2} s^{-1}) is smaller than the soil emission flux due to the fact that the model has not reached a steady state yet for the presented day. However, the 5-day average Rn canopy top flux is nearly identical to the soil emission flux. Figure 1b shows that the calculated canopy top fluxes of O_3, using the 1- and 2-layer grid resolution version, are comparable to that of the 10-layer version. The canopy top flux of O_3 for tropical rain forest is controlled by downward turbulent transport of ozone from the planetary boundary layer (PBL) and surface layer into the canopy and subsequent dry

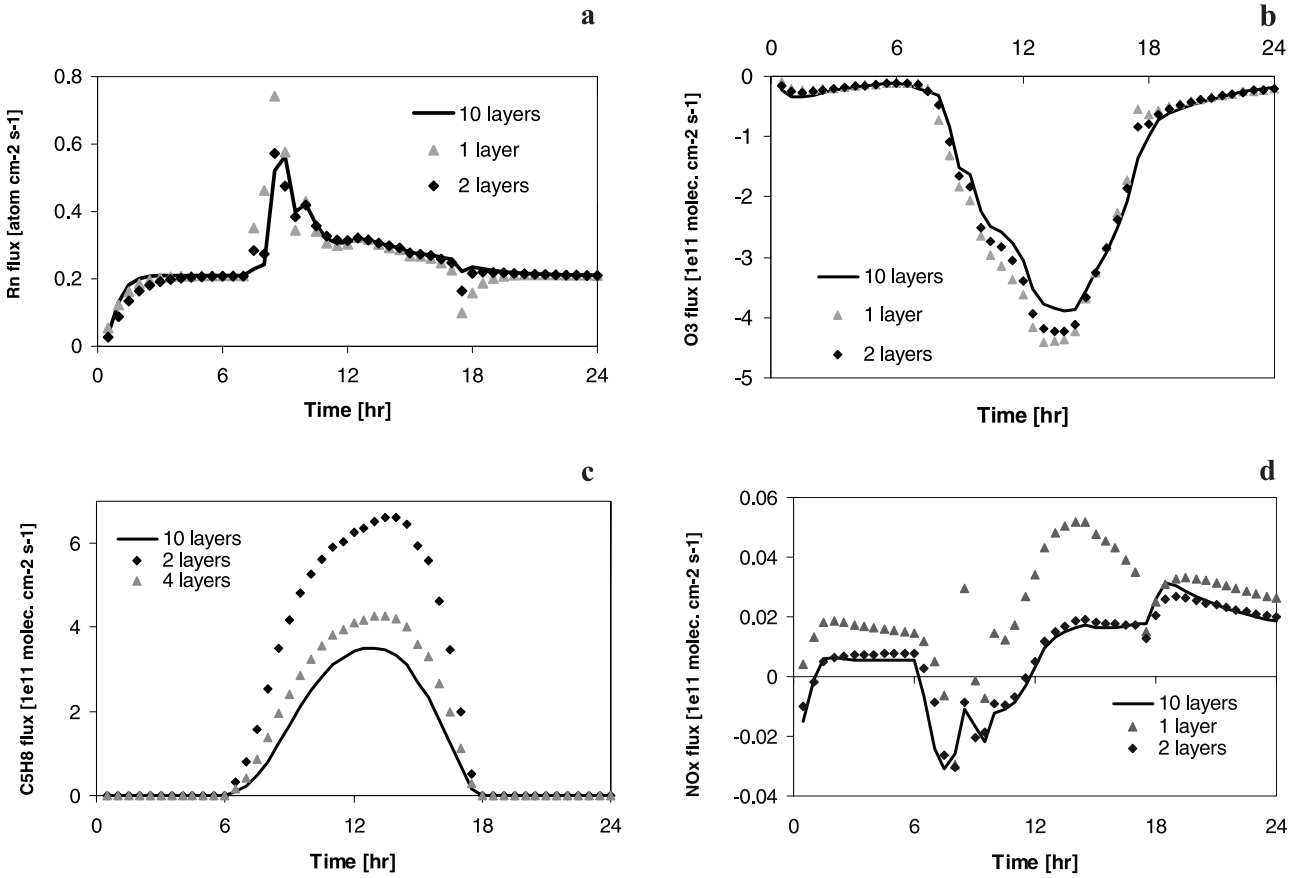

Figure 1. Modeled diurnal cycle of the canopy top flux for tropical rain forest with a canopy height of 30 m and an LAI of 7, for three different vertical resolutions: 10 layers (solid line), 1 layer (triangles) and 2 layers (diamonds); (a) radon canopy flux (atoms cm^{-2} s^{-1}); (b) ozone (10^{11} molecules cm^{-2} s^{-1}); (c) isoprene (10^{11} molecules cm^{-2} s^{-1}) with the triangles referring to 4 layers; and (d) NO_x (10^{11} molecules cm^{-2} s^{-1}).

deposition. Maximum daytime dry deposition velocities are about 2 cm s^{-1}. The similarity of the modeled canopy top fluxes for the three model versions suggests that dry deposition and turbulent transport are quite insensitive to the selected vertical resolution. Hence, it is expected that the big leaf approach calculates similar deposition fluxes as the biosphere model (see section 4.2). Figure 1c shows that the calculated canopy top fluxes of isoprene are highly sensitive for the vertical grid resolution with a >50% larger isoprene canopy top flux for the 2-layer model version compared to the 10-layer model. The 1-layer isoprene canopy top flux is not shown here since it is very similar to that calculated with the 2-layer model version. The large sensitivity for the vertical resolution is mainly due to impact of the discretization of the vertical radiation profiles on the simulated emission strength. There is a strong radiation gradient close to the canopy top, which requires a relative high vertical resolution in the canopy crown. Figure 1c also shows the isoprene canopy flux distinguishing 4 layers and a subsequent interpolation of the calculated emission flux to 2 layers, which yields an isoprene emission flux that deviates less than 20% from the emission flux in the 10-layer model version. Figure 1d shows the modeled diurnal cycle of NO_x, which is controlled by biogenic emissions (we used an NO emission flux of $8.9 \cdot 10^9$ molecules cm^{-2} s^{-1}, see also section 4.1), dry deposition, chemistry and turbulent transport. The complexity of the interactions between these processes results in a bidirectional canopy top flux. It is shown that representing the canopy by one single layer results in an overestimation of the canopy top NO_x flux throughout the day compared to that calculated with the 10-layer resolution. It is also shown that by distinguishing two layers the canopy top NO_x flux is very similar to that calculated by the high-resolution vegetation model.

[16] In summary, the sensitivity of the four trace gases for the selected vertical resolution suggests that we need to distinguish at least two canopy layers to resolve the atmosphere-biosphere trace gas exchange adequately. These two layers are hereafter referred to as the crown and canopy-soil layer. The results also indicate that simulations of isoprene emissions require a higher resolution, being fairly well represented by a four-layer model and the subsequent interpolation of the emission flux to the crown and canopy-soil layer.

3.2. Temporal Resolution

[17] The model integrations shown in the previous section were performed using a time step of 10 seconds. However, since the atmosphere-biosphere model will be implemented in a global model, trace gas exchange processes will be

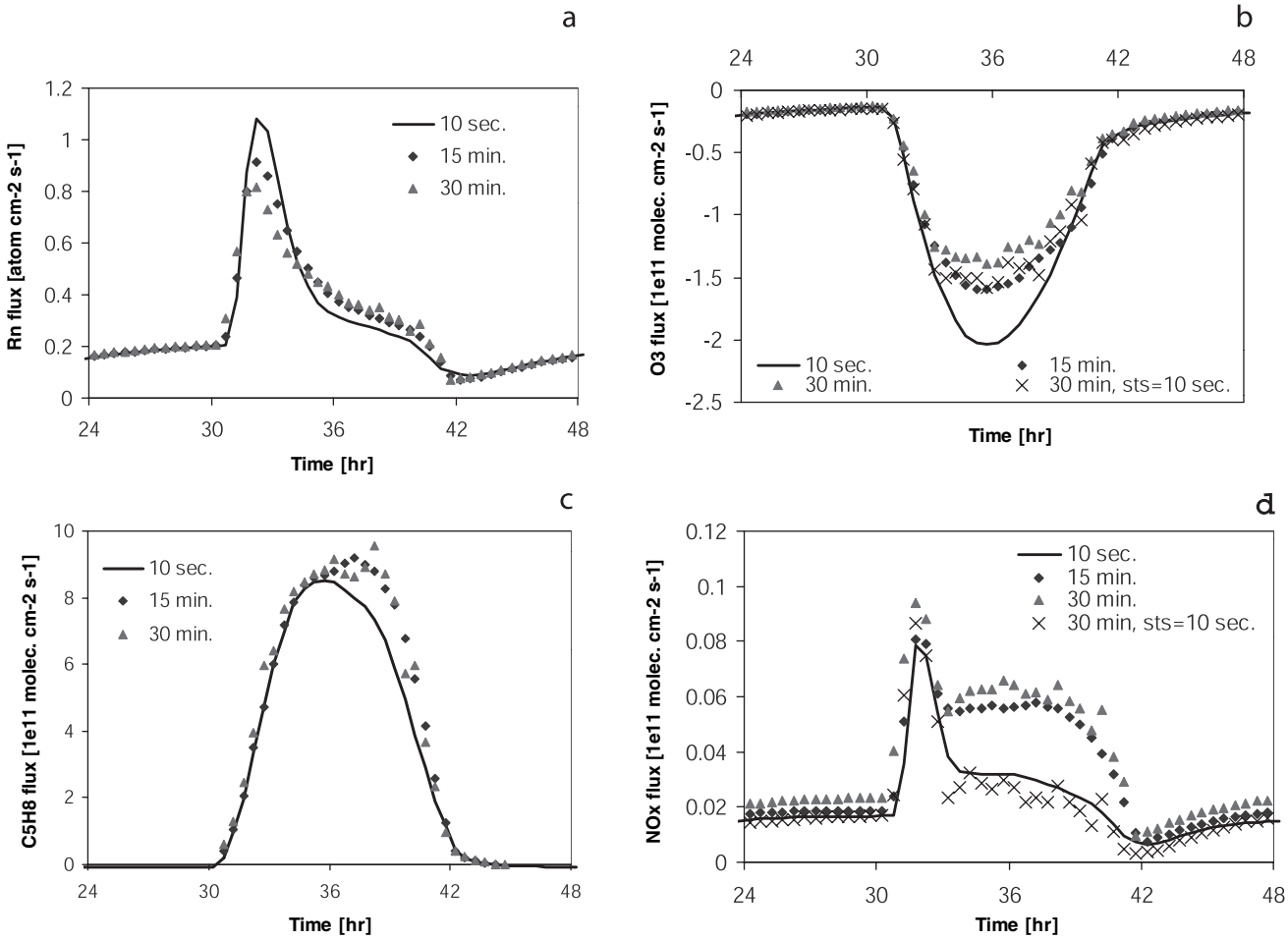

Figure 2. Modeled diurnal cycle of the canopy top flux for a tropical rain forest with a canopy height of 30 m and an LAI of 7, distinguishing two equidistant canopy layers, for three different temporal resolutions: 10 seconds (solid line), 15 minutes (diamonds) and 30 minutes with (crosses) and without (triangles) sub time step (sts); (a) radon canopy flux (atoms cm^{-2} s^{-1}); (b) ozone (10^{11} molecules cm^{-2} s^{-1}); (c) isoprene (10^{11} molecules cm^{-2} s^{-1}); and (d) NO_x-family (10^{11} molecules cm^{-2} s^{-1}).

resolved at a time step of about 15–30 minutes depending on the model version used (T30 or T63 triangular truncation). However, it is not legitimate to consider the turbulent (and convective) transport of NO, NO_2, NO_3, N_2O_5, and HNO_4 separately in a model with a time step larger than 15 minutes since there is a large flux divergence at the "sub" time step scale due to rapid chemical transformations. Therefore the flux-gradient relationships, developed to describe the turbulent transport of inert trace gases, cannot be used to calculate the vertical turbulent fluxes of these reactive species [*Fitzjarrald and Lenschow*, 1983; *Kramm*, 1989; *Gao et al.*, 1991; *Vilà-Guerau de Arellano and Duynkerke*, 1995; *Galmarini et al.*, 1997]. However, the commonly applied approach in models with a time step larger than the chemical timescale is to consider the transport of the so-called NO_x-"family" (in this work defined as NO, NO_2, NO_3, $2 \times N_2O_5$, and HNO_4). This is based on the assumption that the NO_x family can be treated as a conserved chemical species on a timescale of about 30 minutes. In addition to the chemical flux divergence, the timescale of emissions and dry deposition may be of the same order as the turbulence timescale, thereby also causing a flux divergence. For a tropical rain forest canopy of 30 m height and a daytime O_3 deposition velocity of 2.5 cm s^{-1} [*Fan et al.*, 1990], and assuming that dry deposition occurs mostly in the canopy crown, the deposition timescale is about 10 minutes. Therefore, such processes cannot be modeled accurately with a time step as large as 30 minutes. To remove potential numerical inaccuracies, the turbulent and dry deposition timescales are calculated separately from the thickness of the canopy layers and the eddy diffusivity and dry deposition velocity, respectively. The "sub" time step is taken as 10% of the smallest timescale. Consequently, the dry deposition, emissions and the turbulent exchange between the two canopy layers and the surface layer are resolved for the number of sub time steps within each time step. Note that the applied criterion to derive the sub time step has been selected rather arbitrary from trial and error analysis. Moreover, rather than calculating the dry deposition fluxes of the individual NO_x species, we calculate the dry deposition flux of NO_x as a weighted average of the deposition velocities of the individual species and their relative contribution to the NO_x concentration.

[18] In the original version of the implemented chemistry scheme, emissions, dry deposition, and turbulence are

resolved using an operator splitting procedure. However, because of the controlling role of dry deposition, emissions and turbulence for several reactive trace gases under specific conditions we have removed the operator splitting and resolve the coupled differential equations of the vegetation model with a noniterative implicit Eulerian Backward Integration solver.

[19] Since we are particularly interested in studying the sensitivity of the chemistry calculations to the time step we have only considered turbulent transport, dry deposition, emissions and gas phase chemistry. Convective transport and aqueous phase chemistry have been ignored due to the sensitivity of cloud processes to the time step, whereas we used fixed nocturnal and daytime vertical profiles for the eddy diffusivity. The daytime profiles have been scaled with the net radiation to prevent an instantaneous transition after sunrise from the nocturnal to the daytime profile. Figures 2a, 2b, 2c, and 2d show the calculated Rn, O_3, C_5H_8 and NO_x canopy top fluxes for a tropical rain forest, distinguishing the crown and canopy-soil layer, and using a time step of 10 seconds, 15 and 30 minutes. Note that in contrast to Figures 1a–1d, Figures 2a–2d show the simulated fluxes of the second day of a 2-day simulation, not considering convection and using fixed profiles for the eddy diffusivity, which explains the differences between the fluxes shown in Figures 1a–1d and 2a–2d. For Rn, largest differences in the canopy top flux occur shortly after sunrise at the onset of turbulent mixing. This can largely be explained by the representation of the transition of the stable nocturnal to the unstable daytime mixing regime by the semi-implicit algorithm for turbulent exchange of ECHAM [*Deutsches Klimarechenzentrum* (*DKRZ*), 1992]. Figure 2b shows a significant reduction of the canopy top flux of O_3 of about 40% for the 30-minute model integration compared to the 10-second model integration. Applying the sub time step (hereafter referred to as STS) increases the downward flux but does not remove the bias. Analysis of the calculated O_3 concentration profiles indicates that the underestimation of the canopy top flux is due to limited downward transport of O_3 from the PBL to the surface layer. The daytime calculated O_3 gradient between the surface layer and the layer aloft is about 4 ppbv for the 30-minute integration and about 1 ppbv for the 10-second integration. Reducing the time step of the SCM from 30 to 15 minutes shows an increase of the O_3 canopy top flux with a maximum noontime deposition flux that deviates less than 20% from the 10-second maximum flux of $2 \cdot 10^{11}$ molecules cm^{-2} s^{-1}. Figure 2c shows that the calculated isoprene canopy top fluxes are not very sensitive to the applied time step. The afternoon C_5H_8 canopy top flux of the 30-minute time step integration is about 15% larger compared to the 10-second model integration. Finally, in Figure 2d the comparison between the model resolved NO_x canopy top flux for the 10 second integration and the 30 minute integration is shown. For the 30-minute integration the NO_x canopy top fluxes with and without applying the STS are shown. There is good agreement between the model resolved NO_x canopy top flux for the 10-second integration and the 30-minute STS integration, whereas the NO_x canopy top flux for the non-STS integration is overestimated throughout the day. This is explained by an underestimation of the NO_2 dry deposition for the non-STS calculations. Similar to ozone, there are also differences between NO_x concentrations calculated by the 10-second and 30-minute STS model integrations, with most pronounced differences in the early morning after the onset of the mixing. Interpretation of the calculated process tendencies shows that these differences are basically due to differences in the turbulent mixing and not due to differences in the calculated chemistry for the 10-second and 30-minute integrations. This suggests that there is only a small influence of a misrepresentation of the ozone surface layer concentrations on the NO_x concentrations and fluxes through the chemistry.

[20] We conclude that a 2-layer version and a 30 minute time step, considering sub time steps in the coupled differential equations for turbulent transport, dry deposition and emissions of the EBI solver, is generally sufficient to resolve the canopy top fluxes for a selection of trace gases. However, for fast depositing species such as ozone, the canopy top fluxes are sensitive to the model representation of turbulent transport between the PBL and the surface layer for a time step larger than the dry deposition timescale. The 2-layer version of the vegetation model has been implemented in the SCM for a model evaluation that is presented in the next section. A schematic overview is shown in Figure 3, with the 2-layer vegetation model being used to calculate the canopy top fluxes for the vegetation and wet skin fraction. We emphasize that the atmosphere-biosphere model only calculates trace gas concentrations and fluxes and does not consider explicitly the transfer of momentum, heat and moisture within the canopy. For the latter, the surface fluxes are calculated in the SCM according to the "big leaf" approach. The thickness of the equidistant crown and canopy-soil layer ranges from 0.5 to about 15 m, dependent on the canopy height. We only consider canopy interactions for a canopy height larger than 1 m.

4. Model Evaluation

4.1. Comparison with Observations

[21] We have evaluated the modeled trace gas fluxes and concentrations of the 2-layer vegetation model for three surface cover types; tropical rain forest in Brazil [*Bakwin et al.*, 1990a], deciduous forest in the northeastern USA [*Munger et al.*, 1996] and subarctic taiga woodland in Canada [*Bakwin et al.*, 1994], for which detailed observations are available. Moreover, these sites reflect a rather wide range of meteorological and biogeochemical conditions, which indicates the capability of the model to calculate the trace gas exchanges on a global scale. We largely focus on NO_x since we use the vegetation model to study the effect of the surface cover on NO_x emission fluxes on a global scale, as presented by *Ganzeveld et al.* [2002]. We have also compared the ozone fluxes and concentrations since they provide valuable information about dry deposition, chemistry and vertical turbulent transport processes. Moreover, we have included the surface net radiation, energy partitioning and turbulence in our analysis since the representation of these processes will help explaining any disagreement between the calculated and observed concentrations and fluxes. The SCM has been initialized using ECHAM4 vertical profiles of wind speed, temperature, and moisture and surface properties for the grid cell that resemble the location of the measurement sites. Any

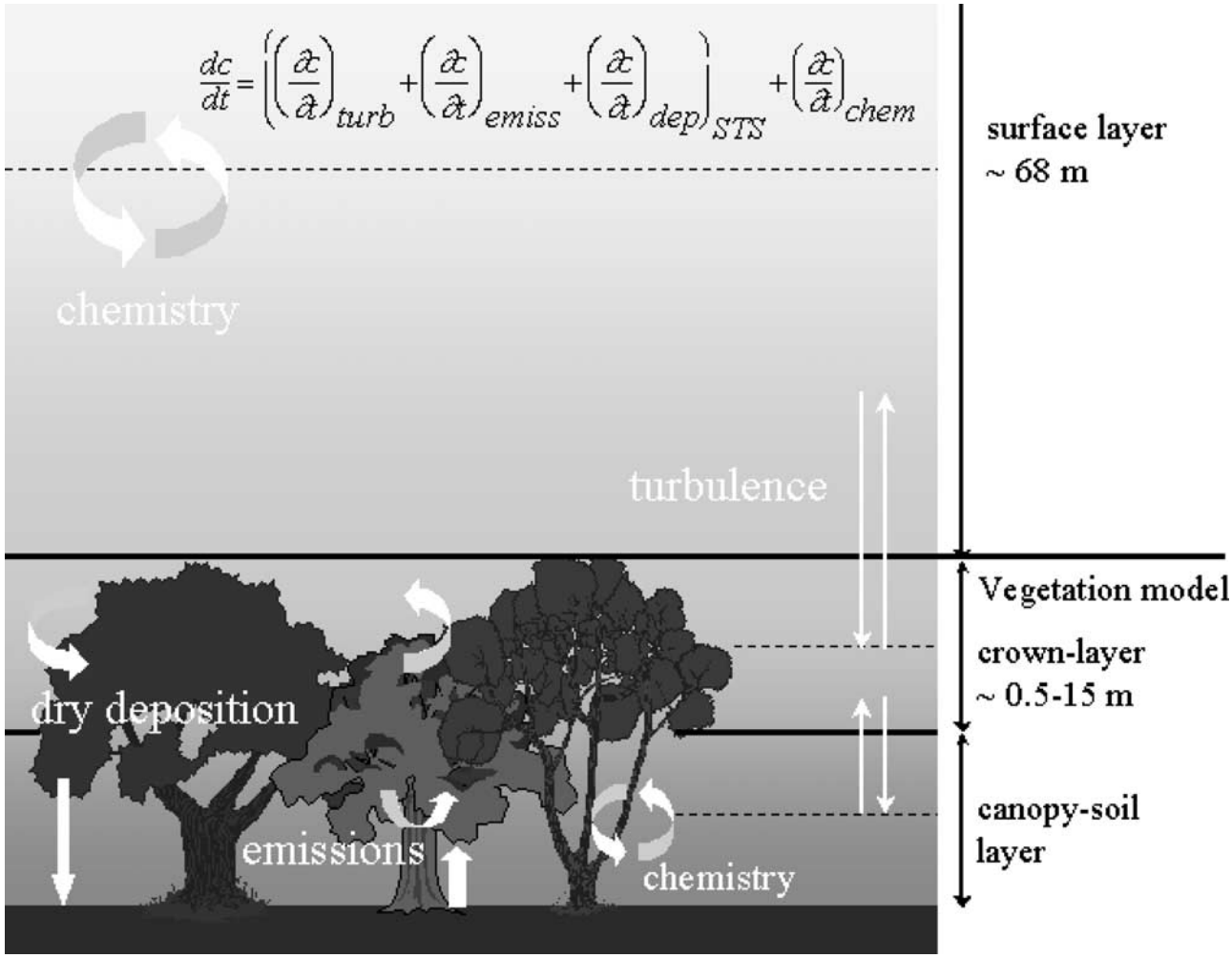

Figure 3. Implementation of the 2-layer vegetation model in the SCM (and ECHAM), with a typical surface layer height of ~68 m. The contribution of biogenic emissions, dry deposition, and turbulence to the concentration changes at the reference height of the canopy layers and surface layer (dotted lines) are calculated using the STS, whereas chemistry calculations use the time step of the SCM (or ECHAM).

adjustment of the modeled physical and dynamical processes, e.g., prescribing the surface net radiation or temperature, is minimized since it introduces inconsistencies between modeled processes. Adjustments that have been made in this work, to ensure a fair comparison between the model and the observations, are the optimization of the surface cover properties and initial vertical profiles. Simulations have been performed for five days, which requires the use of a fixed geostrophic wind speed and direction in the free troposphere to avoid a decrease in the calculated wind speeds throughout the simulation due to the continuous momentum exchange.

[22] The observations over the deciduous forest and taiga woodland indicate that the trace gas concentrations are influenced by the advection of polluted air from nearby anthropogenic sources [*Bakwin et al.*, 1994; *Munger et al.*, 1996]. The observations at the tropical forest site generally reflect a pristine atmospheric composition but the influence of advection of pollution, likely originating from the nearby Manaus urban area, is visible in the NO_y observations [*Bakwin et al.*, 1990b]. Monthly average anthropogenic emissions are considered in the model but these may differ substantially from the local influence of anthropogenic emissions during the observations. In addition to the contribution of primary anthropogenic emissions of NO_x, the O_3 surface layer concentrations are also controlled by advection of photochemically produced O_3 over the source regions. Initial model analyses using the monthly mean anthropogenic emissions showed that the model calculates small day-to-day variations in the fluxes and concentrations over and within the deciduous forest whereas the observations [*Munger et al.*, 1996] showed large differences (>40 ppvb O_3). Not considering these large day-to-day variations in the model calculations results in a serious misrepresentation of the calculated O_3 fluxes and concentrations within the canopy. Therefore, we do not use the monthly mean anthropogenic NO_x emission but have forced the model calculated O_3 and NO_2 surface layer concentrations toward the observed concentrations for the deciduous forest and taiga woodland sites. Actually, constraining the surface layer concentrations using observed concentrations can be interpreted as adding an advection term to the model. The observed O_3 and NO_2 concentrations show rather large fluctuations on a timescale of less than an hour. A sensi-

tivity analysis indicates that in order to reproduce the observed concentration fluctuations a relaxation coefficient of $\sim 10^{-2}$ s^{-1} is required, which implies the use of a time step shorter than 100 seconds. Moreover, since NO_2 or NO_y fluxes have been observed, and not of NO_x, the explicit calculation of the fluxes of individual species of the NO_x family is required, which can only be done for a time step on the order of seconds. Therefore, we use a time step of 10 seconds for the model evaluation instead of the 30 minute time step of ECHAM, also since it is expected that the 10 second and 30 minute integrations yield rather similar calculated trace gas fluxes and concentrations, as has been shown in the previous section. To allow the model to calculate trace gas concentrations and fluxes consistent with the modified surface cover properties, model results starting at the second day are used for the evaluation.

4.1.1. Tropical Rain Forest, Brazil

[23] For a comparison of the observed and modeled O_3 and NO_x canopy top fluxes and concentrations over and within tropical rain forest we have used observations collected during the ABLE-2B campaign, April and May 1987, at the Ducke Forest Reserve near Manaus, Brazil [*Bakwin et al.*, 1990a; *Fan et al.*, 1990; *Fitzjarrald et al.*, 1990]. More recently, the LBA-EUSTACH field campaigns have been conducted in Brazil (M. Andreae et al., Toward an understanding of the biogeochemical cycling of carbon, water, energy, trace gases and aerosols in Amazonia: An overview of the LBA-EUSTACH experiments submitted to *Journal of Geophysical Research*, 2002). However, these data were not yet available for the present model comparison. Future work on model development and evaluation will include the results of these campaigns.

[24] The observations at the Ducke Forest Reserve generally reflect a pristine atmospheric composition indicated by NO, O_3 and CO surface layer concentrations as low as 10 pptv, 6 ppbv and 80 ppbv, respectively [JW90, and references therein]. Here we show a comparison of modeled fluxes and concentrations for a 5-day model integration starting at May 1. Unfortunately, direct flux measurements are restricted to ozone. The NO_y flux has been derived using the observed NO_y concentrations and prescribed vertical exchange velocities, which have also been used in a one-dimensional photochemical model to calculate the NO_x flux [JW90]. These vertical exchange velocities have been derived from observed vertical concentration profiles and fluxes of O_3, Rn and CO_2 throughout the PBL and within the canopy. The canopy structure is defined by a complete vegetation cover expressed by a vegetation fraction of 1, an LAI of 7 and a canopy height of 30 m. The leaf area density profile reflects a vertical biomass distribution with the maximum amount of biomass in the canopy crown [*Fan et al.*, 1990]. We have used a surface roughness of 2 m, estimated from the canopy characteristics according to *Raupach* [1994]. Modeled and observed micro-meteorological parameters for this site are presented in Table 1. The maximum model calculated net radiation (R_n) of about 450 W m^{-2} is smaller then the observed net radiation [*Fan et al.*, 1990; *Roberts et al.*, 1990]. This underestimation of net radiation is associated with a somewhat larger calculated cloud cover (CC) of about 0.9 compared to an observed CC of 0.7. The model reproduces the observed strong extinction of radiation within the canopy [*Shuttleworth*, 1984], indicated by a fraction of leaves exposed to sunlight near the soil surface <2%. According to the model nearly all the available energy at the surface is used for evapotranspiration, which results in the underestimation of the sensible heat flux (H) compared to observations [*Fitzjarrald et al.*, 1990]. It is beyond the scope of this study to address this misrepresentation of the energy partitioning of the tropical rain forest and we refer to a study by *Sellers et al.* [1989] for a more extensive discussion about this issue. Despite the misrepresentation of the surface energy balance, the model reproduces the observed diurnal cycle in the temperature above the canopy with a nocturnal minimum 2-meter temperature (T_{air}) of about 297 K and a maximum 2-meter temperature of about 300 K [*Fan et al.*, 1990, *Roberts et al.*, 1990]. The modeled wind speed (u) at the reference height of the observations, which is derived from the modeled surface layer wind speed using the logarithmic wind profile, is smaller than observed. The overestimation of the latent heat flux by the model is consistent with an overestimation of the surface layer specific humidity (q) of about 19 g kg^{-1} compared to an observed specific humidity of about 15 g kg^{-1} [*Fitzjarrald et al.*, 1990]. In summary, comparison of the calculated and observed micrometeorology for tropical rain forest suggests that there are significant discrepancies, which likely imposes a serious constraint on the interpretation of the trace gas exchanges.

Table 1. Comparison Between Modeled and Observed Micrometeorological Parameters Above and Within Tropical Rainforest, Manaus, Brazil

Parameter	Model	Measurements
R_n [W m^{-2}]	450[a]	~600
CC [0–1]	0.9[b]	~0.7
H [W m^{-2}]	20[a]	~200
T_{air} [K]	297–300 (32 m)	~296–301 (~39 m)
u [m s^{-1}]	0.5–2 (~39 m)	~1.5–2.5 (~39 m)
q [g kg^{-1}]	19 (~53 m)	15 (~39 m)

[a] Five-day average maximum value for the simulation.
[b] Five-day average value. Also indicated are the 5-day average ranges between the minimum nocturnal and maximum daytime values. For the modeled air temperature, wind speed, and specific humidity, the reference height within the surface layer is given in parentheses.

[25] Figure 4 shows the 5-day average diurnal cycle in the modeled and observed O_3 canopy top flux. The modeled maximum O_3 flux is smaller than the observed maximum flux of about $3.5 \cdot 10^{11}$ molecules cm^{-2} s^{-1} [*Fan et al.*, 1990]. The modeled nocturnal fluxes are about $0.4 \cdot 10^{11}$ molecules cm^{-2} s^{-1} and the maximum daytime downward (deposition) flux is about $2.5 \cdot 10^{11}$ molecules cm^{-2} s^{-1}. The underestimation of the O_3 canopy top flux reflects the overestimation of the modeled ozone surface layer concentrations of ~10 ppbv compared to the observed maximum daytime concentrations of about 7 ppbv. Further analysis shows that the underestimation of the O_3 canopy top flux is caused by a too small calculated O_3 dry deposition velocity compared to the observations [*Fan et al.*, 1990]. This is mainly due to a significant fraction of wet vegetation in the model (the so-called wet skin fraction) from convective rainfall interception. It is assumed in our dry deposition model that uptake by a wet canopy is relatively small due to a small removal rate by the wet cuticle and covered leaf stomata [*Wesely*, 1989] (the latter is being discussed more

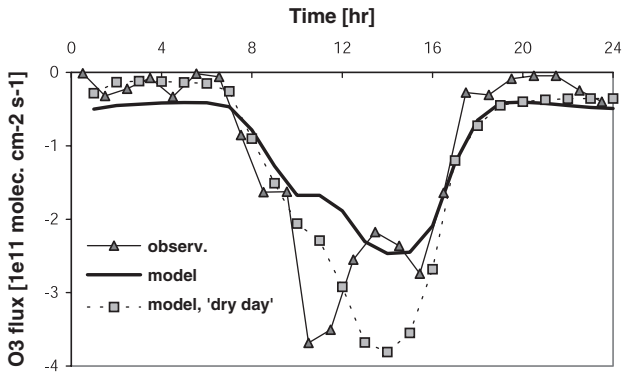

Figure 4. Comparison between the modeled 5-day average diurnal cycle in the canopy top O_3 flux (solid line) (10^{11} molecules cm^{-2} s^{-1}) and the average diurnal cycle in the observed O_3 canopy flux (triangles) over tropical rain forest near Manaus, Brazil, during the ABLE-2B measurement campaign in April and May, 1987. The squares show the modeled diurnal cycle in the O_3 canopy flux for May 1.

extensively in section 5). The observed diurnal cycle in the ozone dry deposition flux and velocity reflects the exchange regime for dry conditions [*Fan et al.*, 1990]. The modeled fraction of wet vegetation increases throughout the five days from a daytime average of about 0.2 during the first two days to more than 0.6 at May 5. The modeled O_3 canopy top flux for May 1, shown in Figure 4 by the dashed line, agrees better with the observations. The maximum modeled O_3 dry deposition velocity for May 1 of about 2 cm s^{-1} compares well with the observed maximum O_3 dry deposition velocity [*Fan et al.*, 1990]. Despite the relatively large canopy top fluxes for the dry compared to the wet days, the difference in the daily average surface layer concentrations during the 5-day integration is small. The modeled daytime concentration of about 10 ppbv in the surface layer is also controlled by the downward convective transport of about 1 ppbv/hr of ozone to the surface layer. Simulations without considering the convective transport yield surface layer concentrations as low as 6 ppbv in the afternoon, which agrees well with the observed surface layer concentrations. This suggests that the model overestimates the convective downward transport of O_3. The model reproduces the nocturnal decrease in the O_3 surface layer concentrations. However, the observations show a rapid decrease shortly after sunset from 6 ppbv down to about 3 ppbv, whereas a slower but continuous depletion of the modeled nocturnal O_3 concentration takes place throughout the night. Observations of nocturnal O_3 dry deposition velocities by *Fan et al.* [1990] are as large as 0.5 cm s^{-1}. These relatively large removal rates are likely related to the observed nocturnal exchange events between the surface layer and the canopy [*Fitzjarrald and Moore*, 1990]. Moreover, the nocturnal O_3 flux is expected to be modified by reactions with NO emitted by the soil [*Bakwin et al.*, 1990b]. It remains an open question to what extent the intermittent nocturnal turbulent exchange or other mechanisms, e.g., chemical destruction by NO, are responsible for the observed rapid decrease after sunset.

[26] Since the soil emission algorithm is constrained by the observed NO emission flux of $8.9 \cdot 10^9$ molecules cm^{-2} s^{-1} [*Bakwin et al.*, 1990b], we only show in Figure 5 the modeled diurnal cycle of the canopy top NO_x fluxes and the calculated flux by JW90. The presence of a wet canopy also leads to a large overestimation of the canopy top NO_x fluxes compared to the estimate by the JW90 model. There is reasonable agreement between the modeled NO_x fluxes for May 1, although the SCM afternoon fluxes are still larger compared to the NO_x fluxes calculated by the JW90 model. The SCM nocturnal canopy top flux of about $1 \cdot 10^9$ molecules cm^{-2} s^{-1} on the 1st of May is similar to the flux calculated by the JW90 model, whereas the 5-day average nocturnal flux calculated by the SCM is $3 \cdot 10^9$ molecules cm^{-2} s^{-1}. Differences in the nocturnal exchange fluxes determine the early morning burst of NO_x into the surface layer due to its accumulation within the canopy during the night. The observations show a nocturnal NO accumulation within the canopy from about 200 up to 500 pptv, and the maximum concentration exceeds 1 ppbv close to the soil surface in the early morning at the onset of turbulent exchange between the canopy and the surface layer [*Bakwin et al.*, 1990b]. In Figure 6 the 5-day average modeled diurnal cycle in the NO concentration of the canopy-soil layer (0–15 m) is shown versus the observed concentrations, which resembles the height-weighted measured concentrations at 0, 3, 6 and 12 m, and the standard deviation. We use the height-weighted measured concentrations instead of using simply the average to avoid being overly influenced by high (NO_x) or low (O_3) concentrations close to the soil surface. The modeled average nocturnal NO concentrations are significantly higher compared to the observations of about 400 pptv. This is partly explained by an underestimation of the nocturnal turbulent exchange between the canopy-soil and the crown layers, indicated by an underestimation of the modeled nocturnal NO concentration in the crown layer of about 100 pptv. Unfortunately there are no observations of NO_2, which would provide information about the chemical conversion of NO to NO_2. The average modeled nocturnal O_3 concentrations of the canopy-soil layer are similar to the observed concentrations at 6 m, about 500 pptv, which indicates that in addition to chemical destruction of NO another sink of NO may be present in the lower canopy, e.g., dry deposition of NO.

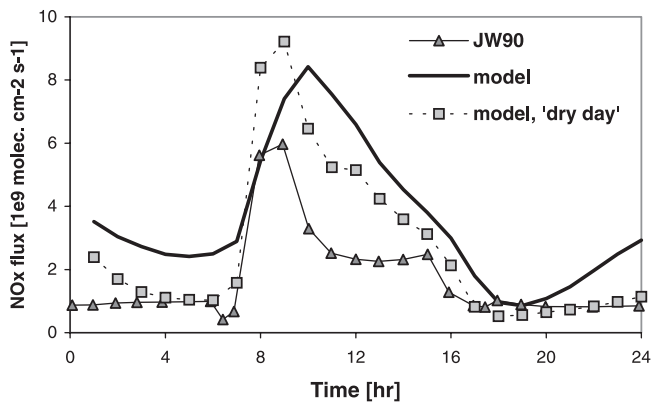

Figure 5. As Figure 4 for NO_x (10^9 molecules cm^{-2} s^{-1}). The JW90 NO_x flux is calculated using a 1-D photochemical model being constrained by estimated eddy diffusivities.

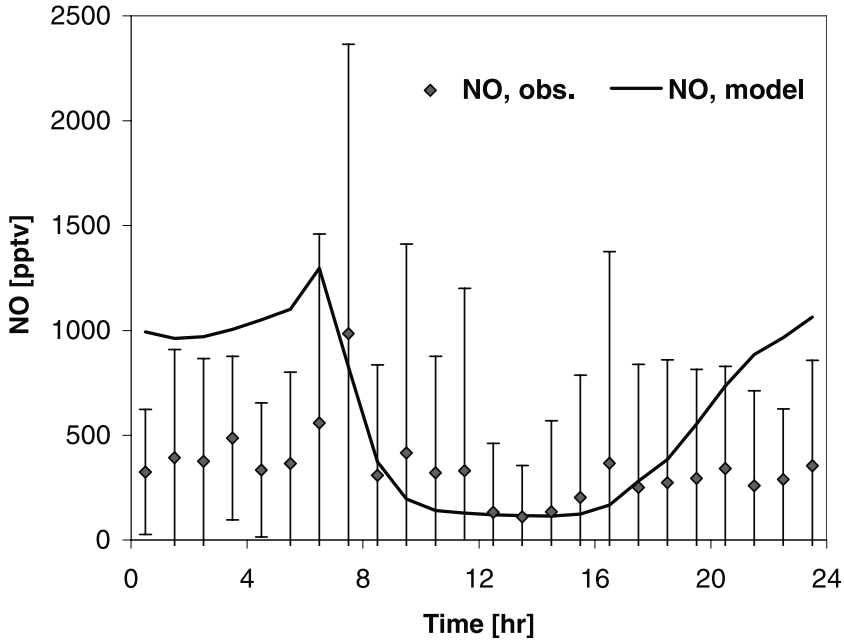

Figure 6. Comparison between the modeled 5-day average diurnal cycle in the canopy-soil layer (csl, 0–15 m) NO concentration (solid line) (pptv) and the average diurnal cycle in the observed NO concentration (diamonds) and standard deviation within a tropical rain forest. The observed NO concentration reflects the height-weighted concentration of the measurements at 0, 3, 6 and 12 m.

However, the 5-day modeled O_3 concentration shows that during the first two days the nocturnal concentrations of the canopy-soil layer are nearly zero, so that NO accumulates up to 2 ppbv. For the last three days the nocturnal O_3 concentrations are larger, resulting in modeled NO concentrations of about 500 pptv, in good agreement with the observed concentrations. The differences in the modeled nocturnal O_3 concentrations are related to a decrease in the nocturnal dry deposition velocity as a result of an increase in the wet skin fraction. This underscores the sensitivity of nocturnal NO_x concentrations and fluxes to dry deposition of NO_x and O_3 associated with small vertical turbulent exchange between the canopy layers during the night.

4.1.2. Deciduous Forest, Northeastern United States

[27] *Munger et al.* [1996] (hereinafter referred to as M96) present 5 years of NO_y and O_3 fluxes and concentrations as well as NO_x measurements at the Harvard forest site. They present a detailed overview of the micro-meteorological and trace gas exchange measurements above and within the mixed deciduous forest at this site from 8–13 September 1992. During the first three days of this period the wind was from the south-west, bringing in warm, moist and polluted air, indicated by observed NO_x and O_3 surface layer concentrations high as 6 and 70 ppbv, respectively. During the last two days a significant decrease in temperature, humidity and O_3 and NO_x concentrations occurred, related to a change to a northerly wind direction. The LAI was about 3.4 and the canopy height 24 m. A vegetation fraction of 1 has been applied and we used an estimated surface roughness of 2 m.

[28] The modeled stomatal resistances are relatively large, applying the initial ECHAM soil wetness since the soil moisture level is close to the permanent wilting point. Unfortunately, no soil moisture measurements have been reported by M96. However, it was concluded that the trees at the measurement site were able to access deep soil moisture (J. Munger, personal communication, 1999) and droughts are relatively short so that the soil moisture deficit never reaches critical levels. This is confirmed by the observed maximum latent heat flux of about 500 W m^{-2} for a maximum net radiation of about 625 W m^{-2} [M96]. Because of the sensitivity of the modeled dry deposition to the soil moisture through the stomatal resistance, we have increased the initial soil moisture content to the field capacity. One additional model constraint is that we have forced the O_3 and NO_2 surface layer concentrations toward the observed concentrations to mimic advection from nearby sources during 8 and 9 September. The comparison between the observed and modeled parameters is presented here by showing the average diurnal cycles for the entire period.

[29] Table 2 shows that the calculated maximum net surface radiation is somewhat smaller than that observed.

Table 2. Comparison Between Modeled and Observed Micrometeorological Parameters Above and Within a Deciduous Forest, Central Massachusetts, USA

Parameter	Model	Measurements
R_n [W m^{-2}]	500[a]	~550
LE [W m^{-2}]	440[a]	~300
H [W m^{-2}]	25[a]	~125
PAR 11 m/top [–]	~0.15	~0.25
T_{air} [K]	289–294 (26 m)	~287–294 (~28 m)
u [m s^{-1}]	1–2.5 (~28 m)	~1.8–2.7 (~28 m)
u_* [m s^{-1}]	0.2–0.6 (~58 m)	0.4–0.8 (~28 m)
q [g kg^{-1}]	11–13 (~58 m)	9–12 (~28 m)

[a] Five-day average maximum value for the simulation.

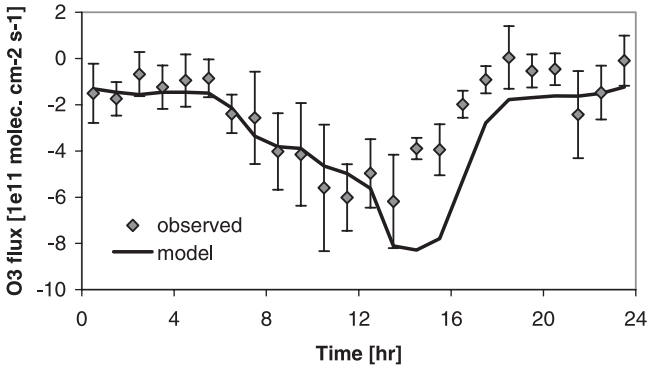

Figure 7. Comparison between the modeled 5-day average diurnal cycle of the canopy top O_3 flux (thick solid line) (10^{11} molecules cm^{-2} s^{-1}) and the average diurnal cycle in the observed O_3 canopy flux (diamonds) and standard deviation over a deciduous forest in Massachusetts, USA, from 8–13 September 1992.

The modeled latent heat flux (LE) is overestimated whereas the sensible heat flux (H) is underestimated. Comparison of the modeled and observed fraction of PAR at 11 m to surface layer PAR indicates reasonable agreement with a modeled fraction of about 0.15 versus an observed fraction of about 0.25 [*Moore et al.*, 1996]. The modeled 5-day average air temperature agrees well with the observed temperature, both in absolute magnitude and the diurnal cycle. The modeled daytime friction velocity is somewhat smaller compared to the observations despite the good agreement for the daytime wind speed. During the night the modeled wind speed is smaller than observed, also reflected in a smaller modeled friction velocity. Finally, there is reasonable agreement between the modeled and observed specific humidity with a 5-day average of about 12 g kg^{-1}. Thus the site micrometeorology is fairly well reproduced by the model.

[30] The comparison between the 5-day average modeled canopy top and observed O_3 flux at about 29 m is shown in Figure 7. The model agrees reasonably well with the observations, indicating nocturnal O_3 fluxes of about $-1.5 \cdot 10^{11}$ molecules cm^{-2} s^{-1} and maximum deposition fluxes in the afternoon of about $-6 \cdot 10^{11}$ molecules cm^{-2} s^{-1}. The model calculates a maximum deposition flux in the afternoon whereas the observed peak flux occurs around noon. The 5-day average diurnal cycle of the modeled dry deposition velocity shows an initial rapid increase in the early morning after sunrise to about 0.5 cm s^{-1}, followed by a small decrease before noon due to an increase in the wet skin fraction as a result of convective rainfall. In the afternoon the wet skin fraction decreases, reflected in an increase of the dry deposition velocity to a maximum of about 0.8 cm s^{-1}. This modeled maximum dry deposition velocity is about 0.2 cm s^{-1} larger than that reported by M96, which explains the overestimation of the maximum modeled O_3 canopy top flux. There are no observations of the NO soil emission flux. However, the calculated flux by the YL95 algorithm is compared to the estimate by M96, who used a mass balance method and the observed vertical profiles of ozone and NO within the canopy. Their estimate of $15 \cdot 10^9$ molecules cm^{-2} s^{-1}, representative of midsummer, is twice as large as our model average flux, based on an emission factor of $1.16 \cdot 10^9$ molecules cm^{-2} s^{-1} for a wet soil for a woodland ecosystem according to YL95.

[31] The comparison between the 5-day average diurnal cycle in the observed and the modeled NO_y (NO_x family + HNO_3 + PAN + MPAN + organic nitrate) flux is shown in Figure 8. The modeled daytime NO_y fluxes compare well to the observed fluxes of about $-0.6 \cdot 10^{11}$ molecules cm^{-2} s^{-1}. However, especially in the evening the modeled NO_y fluxes are significantly smaller compared to the observations. Figure 8 also shows the contribution of the NO_x and HNO_3 fluxes to the NO_y flux, indicating that it is largely controlled by the HNO_3 flux, whereas the NO_x flux is smaller than $-0.15 \cdot 10^{11}$ molecules cm^{-2} s^{-1}. The modeled average nocturnal NO_x canopy top flux is downward, being comparable to the soil biogenic emission flux whereas there is an upward daytime NO_x canopy top flux of about half the soil emission flux. The nocturnal NO_x canopy top flux is controlled by dry deposition of NO_2, whereas during daytime there is an upward NO_2 and NO_x flux due the chemical production of NO_2 within the canopy. The fact that the NO_y flux is controlled by the HNO_3 flux explains the large variability in the 5-day average observed NO_y fluxes since the HNO_3 canopy top flux is controlled by turbulent exchange. The explanation for the underestimation of the nocturnal NO_y flux is therefore related to a misrepresentation of the nocturnal turbulent exchange. The 5-day average modeled and observed friction velocity agree reasonable well for the late night and daytime. However, the modeled friction velocity in the evening and early night is significantly smaller than observed, which suggests that the modeled growth of the nocturnal inversion is too fast. The underestimation of the turbulent exchange in the evening is also reflected in the comparison of the modeled and observed NO concentrations of the canopy-soil layer, shown in Figure 9. The observed canopy-soil layer (0–12 m) concentration represents the height-weighted measured con-

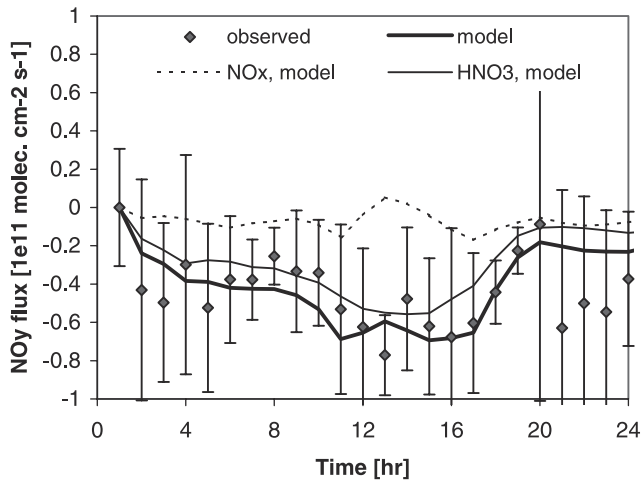

Figure 8. Modeled 5-day average diurnal cycle of the canopy top NO_y flux (solid line) (10^{11} molecules cm^{-2} s^{-1}) and the observed canopy flux (diamonds) and standard deviation over a deciduous forest. Also shown are the modeled NO_x (dashed line) and HNO_3 flux (thin solid line).

centrations at heights of 0.3, 0.8, 4.5 and 7.5 m. The modeled nocturnal NO concentrations are about 100 pptv compared to observed concentrations of about 20 pptv. Underestimation of the chemical destruction is not likely the cause of the overestimation since nocturnal O_3 concentrations are as large as 10 ppbv. There is reasonable agreement between the modeled and observed surface layer NO concentrations with maximum concentrations up to about 500 pptv in the early morning due to the photo-dissociation of NO_2. The modeled NO_2 concentrations in the canopy, not shown here, are in good agreement with the observations. The maximum concentration is about 3 ppbv around midnight, after which there is a decrease to about 2 ppbv in the early morning, reaching minimum concentrations of about 700 pptv around noon.

[32] The comparison between the modeled and observed O_3 concentrations within the canopy, shown in Figure 10, again underscores the role of nocturnal turbulent exchange within the canopy. The observed canopy-soil layer (0–12 m) concentration again represents the height-weighted measured concentrations at heights of 0.3, 0.8, 4.5 and 7.5 m whereas the crown layer (12–24 m) concentration represents the height-weighted measured concentration at 12.7 and 18.3 m. There is good agreement between the modeled and observed O_3 concentrations in the crown layer. However, especially during the night the modeled concentrations in the canopy-soil layer are about 10 ppbv smaller than observed. A striking feature is that largest differences between the modeled and observed concentrations occur in the evening after which there is actually an increase in the modeled concentrations at night due to downward turbulent transport. Further analysis shows that relatively large destruction of ozone by dry deposition takes place after sunset, which is not balanced by turbulent transport. Maximum destruction rates up to 5 ppbv hr^{-1} are calculated, which explains the rather large decrease in the modeled O_3 canopy-soil concentrations. This highlights, in addition to the results for tropical rain forest, the sensitivity of the atmosphere-biosphere trace gas exchange to the nocturnal turbulent exchange. Moreover, it shows the sensitivity to the transition from day to night conditions by the timing of the decoupling between the surface layer and the canopy, and significant changes in the other canopy processes such as dry deposition.

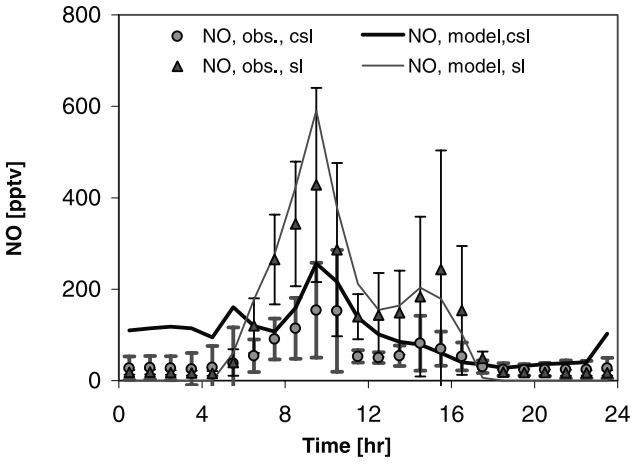

Figure 9. Comparison of the modeled 5-day average diurnal cycle of NO (pptv) in the canopy-soil layer (csl, 0–12 m, solid line) and the surface layer (sl, 24– ~90 m, thin solid line) with the average diurnal cycle of the observed NO concentrations within the canopy (dots) and the standard deviation, and above a deciduous forest (triangles). The observed within-canopy NO concentration reflects the height-weighted concentration measured at 7.5, 4.5, 0.8 and 0.3 m whereas the observed surface layer concentration reflects the measurements at 29 m and 24.1 m.

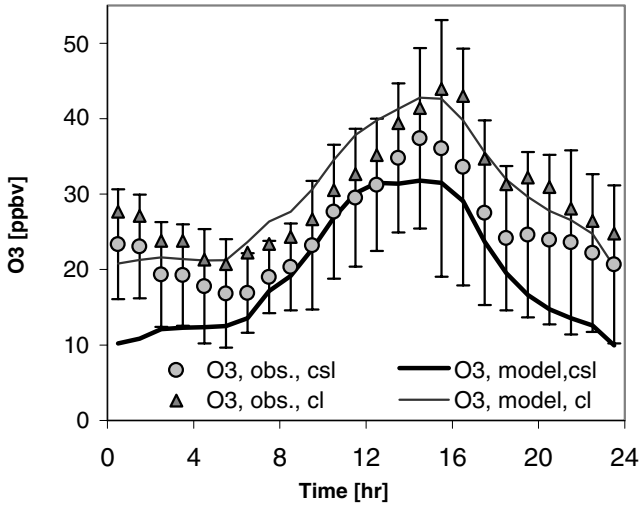

Figure 10. Comparison of the modeled 5-day average diurnal O_3 cycle (ppbv) of the canopy-soil layer (csl, 0–12 m, solid line) and the crown layer (cl, 12–24 m, thin solid line) with the average diurnal cycle of the observed O_3 concentrations within the canopy-soil layer (dots) and the standard deviation, and the concentrations within the crown-layer of deciduous forest (triangles). The observed canopy-soil layer O_3 concentration reflects the average concentration of the measurements at 7.5, 4.5, 0.8 and 0.3 m whereas the observed crown layer O_3 concentration reflects the measurements at 18.3 m and 12.7 m.

4.1.3. Taiga, Canada

[33] Observations of NO_y and O_3 concentrations and fluxes over a woodland in Canada have been made during June–August, 1990, as part of the Arctic Boundary Layer Expedition (ABLE-3B) [*Bakwin et al.*, 1994; M96]. The vegetation type was a lichen woodland with an average canopy height of 6.5 m. The inferred LAI for this site in August is 3.3. We have applied a surface roughness of 0.45 m based on an inferred daytime surface roughness of 0.7 m and a nocturnal surface roughness of 0.2 m [*Fitzjarrald and Moore*, 1994]. The vegetation fraction of ECHAM of about 30% for this site is comparable to the canopy coverage calculated from the observed tree density of 616 stems/ha and an average crown basal diameter of 2 m [*Fitzjarrald and Moore*, 1994]. The remaining 70% of bare soil surface in the model is assumed to represent the surface cover properties of the lichen mat at the measurement site. Using the initial vertical profiles and surface properties derived from the ECHAM model yields a Bowen ratio (ratio of sensible to latent heat flux, β) of about 0.5 compared to an observed one of 2.5–3 [*Fitzjarrald and Moore*, 1994]. This underestima-

Table 3. Comparison Between Modeled and Observed Micrometeorological Parameters Above and Within a Lichen Woodland, Schefferville, Canada[a]

Parameter	Model	Measurements
R_n [W m^{-2}]	400[b]	450
H [W m^{-2}]	200[b]	200
β [−]	2.9	2.5–3
T_{air} [K]	279–285 (∼39 m)	280–286 (∼30 m)
u [m s^{-1}]	3.3–5.3 (∼30 m)	2.1–4.8 (∼30 m)
u_* [m s^{-1}]	0.25–0.55 (∼39 m)	0.1–0.45 (∼30 m)

[a] The Bowen ratio is the 5-day average daytime value.
[b] Five-day average maximum value for the simulation.

tion of the modeled sensible heat flux is also clearly reflected in an underestimation of the calculated PBL height and surface layer temperature. The observed PBL height was about 2 km whereas the model resolved PBL reaches a maximum height of 750 m. Reducing the soil moisture by a factor of two (the initial soil moisture level is about 7 cm), improves the agreement between the calculated and observed evaporation, which is only 10% of the potential evaporation. *Fitzjarrald and Moore* [1994] hypothesize that a possible explanation for the relatively small evaporation is a soil water deficit likely due to the very thin, rocky soil at the site. However, there are no observations of soil moisture to confirm this.

[34] We have selected a 5-day period of observations starting on 20 July. The observed daily average air temperature for this 5-day period shows a steady increase from less then 278 K for 20 July up to about 289 K on July 24. This transition can be explained by changes in wind direction and wind speed. Since there is a large difference between the observed and our initial temperature and moisture profiles, we have modified the initial temperature profile such that the initial surface layer temperature resembles the observed air temperature and moisture at the start of the integration.

[35] The comparison between modeled and observed micro-meteorological parameters using the modified initial vertical profiles and soil moisture for this site, and a derived July LAI of 3.8, is shown in Table 3. The 5-day average calculated maximum net surface radiation is about 50 W m^{-2} smaller than observed. The maximum modeled and observed sensible heat fluxes are about 200 W m^{-2}. The improved representation of the energy partitioning using the modified soil moisture is supported by the agreement between the calculated and observed average daytime Bowen ratio. The modeled 5-day average air temperature agrees well with the observations both in absolute magnitude and the diurnal cycle. The daily average increases from about 278 K on July 20 to 286 K on July 25. The calculated and observed daytime wind speed and friction velocity agree reasonable well. However, the modeled nocturnal turbulent mixing is significantly larger compared to the observed turbulence, indicated by a modeled nocturnal friction velocity which is about 0.15 m s^{-1} larger than observed due to an overestimation of the nocturnal wind speed. Thus, similar to that over deciduous forest, the model reproduces the micrometeorology over the taiga woodland fairly well using the modified soil moisture, air temperature and moisture profiles.

[36] A striking feature of the observed oxidized nitrogen concentrations is the small NO_x to NO_y ratio [*Bakwin et al.*, 1994 (hereinafter referred to as B94); M96]. Model calculations indicate that the maximum PAN concentrations do not exceed 125 pptv, whereas the observed NO_y concentrations reach 400 pptv, consistent with the reported PAN/NO_y ratios by B94 (and references therein). This suggests that NO_y mostly consists of other NO_y species such as HNO_3, reaching the site by advection and subsidence of photochemically aged air pollution [B94, M96]. Hence, the model surface layer NO_y and O_3 concentrations have been forced toward the observed concentrations. To distribute the additional NO_y over the contributing species, the observed ratio between NO_x and NO_y of about 0.2 [B94] has been used to adjust the NO_2 and HNO_3 surface layer concentrations.

[37] Figure 11 shows the comparison between the 5-day average modeled and observed O_3 flux at about 30 m. Actually since the surface of this site is not completely covered by vegetation, we show both the modeled canopy top flux and the surface flux. The latter reflects the contribution of the vegetation as well as the bare soil fraction in the trace gas flux and is calculated from the vegetation and bare soil fraction of 30% and 70%, respectively, and the canopy top flux and bare soil dry deposition flux. There is good agreement between the calculated and observed daytime surface fluxes of O_3 with maximum values of about $-2 \cdot 10^{11}$ molecules cm^{-2} s^{-1}. The modeled nocturnal O_3 surface flux, however, is significantly larger than observed, which can be explained by the differences between the modeled and observed nocturnal turbulence intensity. The calculated canopy top flux reflects the exchange fluxes for a complete vegetation cover with the selected canopy characteristics. Hence, the differences between the canopy top flux and surface flux underscores the sensitivity of the resolved O_3 exchange flux to the selected initial fractions of surface cover. The calculated maximum O_3 dry deposition velocity of about 0.3 cm s^{-1} is comparable to that reported by M96.

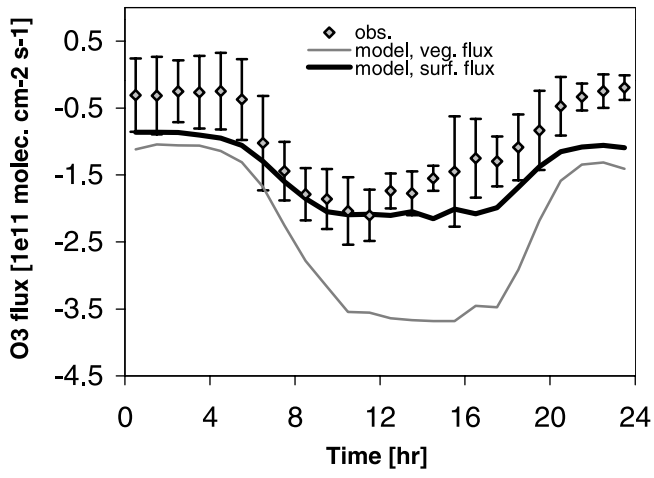

Figure 11. Comparison between the modeled 5-day average diurnal cycle of the O_3 surface flux (solid line) and the canopy top flux (thin solid line) (10^{11} molecules cm^{-2} s^{-1}) and the average diurnal cycle of the observed O_3 flux (diamonds) and standard deviation over a taiga woodland, Schefferville, Canada, from 20–25 July, 1992.

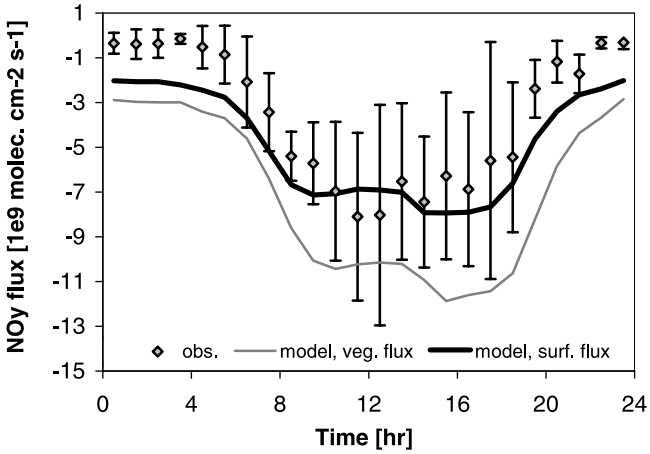

Figure 12. As Figure 11 but for NO_y.

[38] There are no observations of the NO soil emission flux, but it has been inferred using a similar approach as used for the Harvard forest site. The 5-day average modeled NO soil emission flux of about $0.4 \cdot 10^9$ molecules cm^{-2} s^{-1} is similar to the inferred flux for the woodland site between 0 and $1 \cdot 10^9$ molecules cm^{-2} s^{-1} [M96]. The comparison between the 5-day average diurnal cycle in the modeled and the observed NO_y flux is shown in Figure 12. The modeled daytime NO_y surface fluxes agree well with the observations of $-8 \cdot 10^9$ molecules cm^{-2} s^{-1}, whereas the modeled nocturnal NO_y fluxes are larger than observed due to the too strong turbulence intensity. The contribution of the NO_x and HNO_3 fluxes to NO_y is not shown here since NO_x fluxes are as small as $-0.1 \cdot 10^9$ molecules cm^{-2} s^{-1}, which indicates that also for this site the NO_y fluxes are controlled by HNO_3 dry deposition. Since there are distinct differences in the deposition velocities of the different species of NO_y, e.g., HNO_3 and PAN, the agreement between the modeled and observed NO_y fluxes supports the assumption that the advected NO_y largely consists of HNO_3. The daily average downward NO_x canopy top flux of about half the soil biogenic emission flux reflects the NO_2 deposition flux, whereas the daily average NO surface flux is negligible.

[39] Evaluation of the modeled concentrations within the canopy is not straightforward since the modeled within-canopy concentrations reflect the conditions within a fully covered woodland canopy, whereas the observations reflect the concentrations of the canopy environment and the open space between the trees dependent on the mixing conditions. Therefore, we have performed an additional model integration using a vegetation fraction of 1 and a reduced LAI of 1.2 (derived from the 30% vegetation fraction with an LAI of 3.8). The comparison of the modeled and observed O_3 concentrations of the canopy-soil and crown layer is shown in Figure 13. The observed canopy-soil layer (0–3.25 m) concentration represents the height-weighted measured concentrations at heights of 0.05, 0.85 and 2.8 m, whereas the crown-layer (3.25–6.5 m) concentration represents the measured concentration at 6.2 m. There is good agreement between the modeled and observed nocturnal concentrations within the crown-layer whereas the modeled nocturnal canopy-soil concentrations are significantly larger compared to the observations. However, the modeled concentrations are within the 1-σ level, which is largely associated with a strong gradient in the observed concentrations between 0.05, 0.85 and 2.8 m used to construct the average observed canopy-soil concentrations. The observed nocturnal concentrations at 0.85 and 2.8 m are very similar, about 15 ppbv, whereas the nocturnal O_3 concentration observed at 0.05 m is smaller than 5 ppbv, suggesting a strong decoupling close to the soil surface. Note that the 5-day hourly average observed concentrations in the afternoon are biased due to missing data for three of the five days. Therefore we have only sampled the calculated concentrations for those hours for which observations were available. The good agreement indicates that the vegetation concentrations are controlled by the downward turbulent transport of surface layer ozone (which has been adjusted using the observed surface ozone concentrations). Turbulent transport also controls the NO_2 concentrations within the canopy since these are comparable to the surface layer concentrations. Figure 14 shows good agreement between the modeled and observed NO_2 concentrations with minimum calculated concentrations before sunrise of about 35 pptv, with a subsequent continuous increase to a maximum of about 65 pptv after sunset. We only show here the comparison between the canopy-soil layer NO_2 concentrations since the crown-layer and surface layer concentrations are very similar. The modeled maximum daytime NO concentration is about 20 pptv compared to an observed concentration of about 10 pptv. Nocturnal NO concentrations are negligible, as reproduced by the model.

[40] It can be concluded from the model evaluation for the three sites that there is reasonable agreement between the modeled and observed meteorology, adjusting the initial vertical profiles and surface properties, although discrepancies remain, especially concerning the surface energy

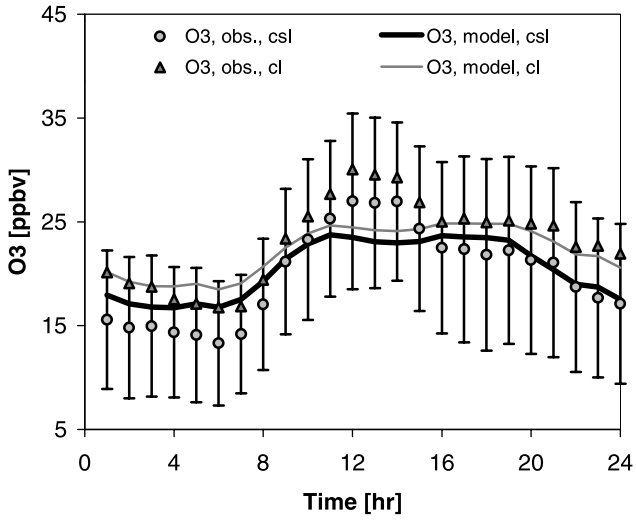

Figure 13. Comparison of the modeled 5-day average diurnal O_3 cycle (ppbv) in the canopy-soil layer (0–3.25 m) (solid line) and the crown layer (3.25–6.5 m) (thin solid line) with the average diurnal cycle of the observed height-weighted O_3 concentration (and standard deviation) at 0.05, 0.85 and 2.8 m (dots) and 6.2 m (triangles) within taiga woodland.

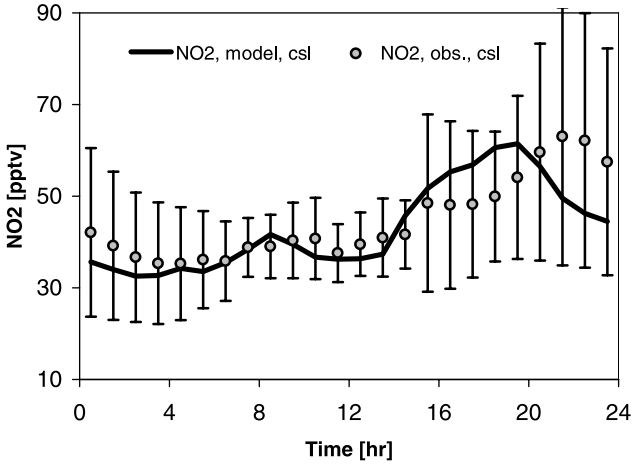

Figure 14. Comparison of the modeled 5-day average diurnal cycle of NO_2 concentrations (pptv) in the canopy-soil layer (0–3.25) (solid line) with the average diurnal cycle of the observed height-weighted NO_2 concentration (and standard deviation) at 0.05, 0.85 and 2.8 m within the canopy (dots).

partitioning. This is basically related to the representation of the stomatal exchange in the SCM, which is sensitive to the selected initial soil moisture conditions. The evaluation of the calculated and observed O_3 and NO_y fluxes and O_3 and NO_x concentrations also shows reasonable agreement for daytime, dry conditions, forcing the calculated surface layer concentrations to the observed concentrations to consider the contribution by advection. The evaluation of the O_3 deposition fluxes for the tropical rain forest has indicated the importance of surface wetness in controlling the dry deposition process. Especially for nighttime conditions, the large sensitivity to the turbulent mixing and removal processes in the canopy, e.g., dry deposition can result in significant discrepancies.

4.2. Biosphere Model Versus Big Leaf Approach

[41] In this section, we compare the modeled NO_x canopy top fluxes of the biosphere model with the net flux of the separate representation of emissions and dry deposition of the big leaf approach, for the same three sites and time of year as presented in the previous section. We emphasize that this comparison shows the differences between different model approaches and does not imply that the presented fluxes calculated by the biosphere model reflect the true fluxes at the three different sites. A main difference between the results presented in this section and those shown in section 4.1 is that here we have applied the ECHAM monthly mean anthropogenic emission fluxes instead of forcing the surface layer concentrations toward the observations.

[42] YL95 introduced a first-order estimate of the decrease in the NO soil emission flux due to within-canopy chemical transformations and dry deposition, expressed by the daily averaged flux escape efficiency, or Canopy Reduction Factor (CRF). Their CRF is an ecosystem dependent parameter calculated from the LAI reflecting the uptake by the cuticle and the Stomatal Area Index (SAI), which represents the active absorption of NO_2 by the leaf stomata during the daytime [*Jacob and Bakwin*, 1991]. To show the influence of using the CRF on the net fluxes of NO_x, the calculations for the big leaf approach have been done with and without the CRF. The simulations have been performed using the ECHAM time step of 30 minutes. Soil emissions are explicitly calculated using the YL95 algorithm. Figure 15 shows the modeled 5-day average diurnal cycle of the canopy top NO_x flux and the net emission and dry deposition flux by the big leaf approach (hereafter referred to as big leaf surface flux) for tropical rain forest. The YL95 canopy reduction factor for tropical rain forest is about 0.25. The relatively small value of the CRF is reflected in the difference between the daily average NO_x flux calculated with the big leaf approach with and without this CRF of 1 and $5 \cdot 10^9$ molecules cm^{-2} s^{-1}, respectively. Clearly, using the CRF improves the description of NO_x exchange fluxes within the canopy compared to the uncorrected big leaf approach, however, discrepancies remain especially concerning the calculated diurnal cycle. The daytime NO_x flux calculated with the big leaf approach with the CRF is comparable to the NO_x flux of the biosphere model with an early morning dry deposition flux and an afternoon emission flux of about $1.5 \cdot 10^9$ molecules cm^{-2} s^{-1}. However, the nocturnal NO_x fluxes are very different with an emission flux of about $1 \cdot 10^9$ molecules cm^{-2} s^{-1} calculated with the big leaf approach, whereas the biosphere model calculates a small NO_x deposition flux. Further analysis indicates that the differences between the nocturnal big leaf and biosphere NO_x fluxes are basically due to relatively small differences between the modeled big leaf and biosphere dry deposition velocities. This shows again the sensitivity of the nocturnal trace gas exchange to the dry deposition process for suppressed turbulent exchange. There is a significant difference in the daily average fluxes of both approaches, indicated by a negligible daily average NO_x flux calculated with the biosphere model, whereas the daily average NO_x flux of the big leaf approach, using the CRF, is about $0.7 \cdot 10^9$ molecules cm^{-2} s^{-1}. However, the smaller canopy top flux of the biosphere model does not result in a smaller surface layer

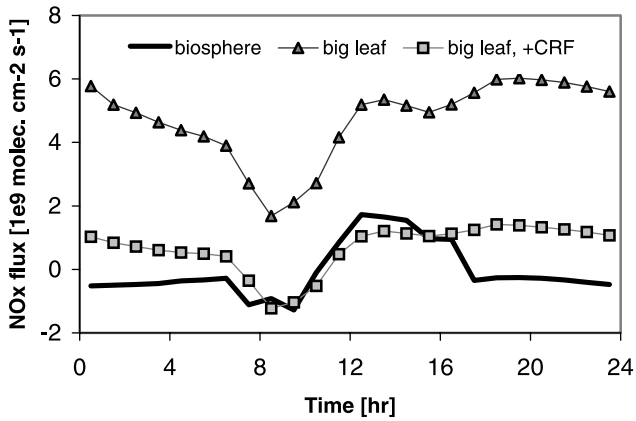

Figure 15. Modeled 5-day average diurnal cycle in the canopy top NO_x flux (solid line) (10^9 molecules cm^{-2} s^{-1}) and the net emission and dry deposition NO_x flux by the big leaf approach, compared with the CRF (squares) and without the CRF (triangles), for tropical rain forest.

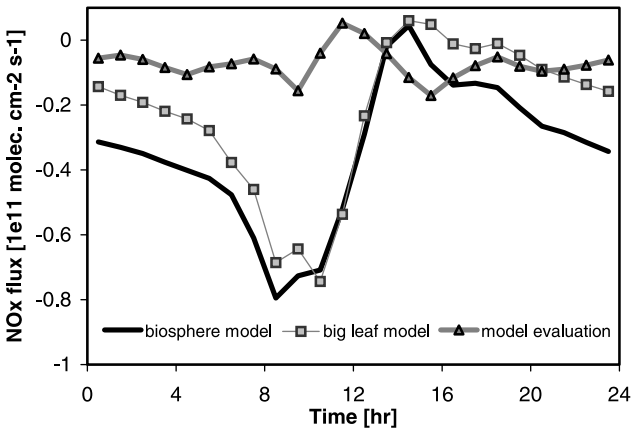

Figure 16. Modeled 5-day average diurnal cycle of the canopy top NO_x flux (solid line) (10^{11} molecules cm^{-2} s^{-1}) and the net emission and dry deposition NO_x flux of the big leaf approach with the CRF (squares) for deciduous forest. Also shown is the canopy top NO_x of the model evaluation (traingles) for the deciduous forest, as presented in Figure 8.

NO_x concentration. The calculated 5-day average NO_x surface layer concentration of the biosphere model of about 250 pptv is generally larger compared to the big leaf approach with maximum differences of about 200 pptv toward the end of the night. This can largely be explained by the decrease in the surface layer concentrations due to dry deposition for the big leaf approach, whereas in the biosphere model the removal by dry deposition occurs within the canopy. These results show that by explicitly considering the processes in the canopy, the canopy top NO_x flux from tropical rain forest is reduced. However, this does not necessarily imply that the surface layer concentrations are reduced as well.

[43] Figure 16 shows the modeled 5-day average diurnal cycle of the canopy top and big leaf surface NO_x flux for deciduous forest with an inferred canopy reduction factor of about 0.6. The NO_x flux for the big leaf approach, without the CRF, is not shown here since it is very similar to the flux calculated by the big leaf approach using the CRF. The canopy top NO_x flux is largely controlled by dry deposition of surface layer NO_x being supplied by an anthropogenic NO_x emission flux in the surface layer of $1.9 \cdot 10^{11}$ molecules cm^{-2} s^{-1}, which is about a factor of 20 larger than the average biogenic NO emission flux. The diurnal cycle in the canopy top NO_x flux reflects the diurnal cycle in concentration gradient between the surface layer and the crown layer and the eddy diffusivity. The gradient is largest during the night due to the continuous contribution of the anthropogenic emission flux to the NO_x surface layer concentration and the suppressed turbulent mixing. There is a decrease in the downward gradient in the morning due to the enhanced turbulent mixing whereas in the afternoon a small upward gradient is calculated resulting in the small emission flux. Maximum fluxes of $-0.7 \cdot 10^{11}$ molecules cm^{-2} s^{-1} occur in the early morning due to an increase in the turbulent mixing and the removal by dry deposition of NO_x that has accumulated in the nocturnal surface layer. The small early afternoon NO_x flux is related to a reduced dry deposition velocity due to the presence of a significant fraction of wet vegetation. Again, small differences between the big leaf and biosphere dry deposition velocities largely explain the differences between nocturnal NO_x deposition fluxes of the biosphere model and big leaf approach. Figure 16 also shows the NO_x flux, calculated for the model evaluation presented in the previous sections, to indicate the difference between NO_x fluxes calculated using the monthly mean emission flux and forcing the surface layer concentrations toward the observations. Especially at night and in the early morning the NO_x deposition fluxes calculated using the monthly mean anthropogenic emission flux are significantly larger compared to the NO_x flux of the model evaluation. This can largely be explained by the nocturnal accumulation of NO_x in the surface layer using the monthly mean emission fluxes, which apparently does not realistically represent the local advection of NO_x from nearby source regions.

[44] Figure 17 shows the calculated 5-day average diurnal cycle of the vegetation model and big leaf surface flux of NO_x, with and without the CRF, for taiga woodland. The inferred CRF for this site is about 0.6 and the anthropogenic NO_x emission flux for this site is $1.3 \cdot 10^9$ molecules cm^{-2} s^{-1} compared to a 5-day average soil biogenic emission flux of about $0.3 \cdot 10^9$ molecules cm^{-2} s^{-1}. The big leaf and biosphere surface flux show a similar diurnal cycle, but the big leaf surface flux is larger than the biosphere surface flux. This is also reflected in the daily average surface fluxes of both approaches with an average deposition flux of $-0.15 \cdot 10^9$ molecules cm^{-2} s^{-1} for the biosphere model and a negligible NO_x flux for the big leaf approach, with and without using the CRF.

[45] It thus follows that for the deciduous forest, with NO_x concentrations being controlled by the continuous supply of NO_x by advection, the big leaf approach calculates similar NO_x surface fluxes as the biosphere model. Differences between calculated NO_x fluxes by the big leaf approach and the biosphere model are largely explained by differences in the dry deposition velocities and not by the canopy interactions. For the tropical rain forest and taiga woodland, where the NO_x burden is controlled by the biogenic emission, there are large differences in the calcu-

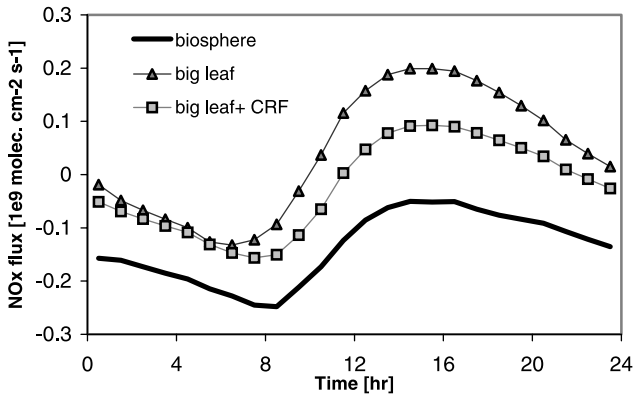

Figure 17. Modeled 5-day average diurnal cycle of the canopy top NO_x flux (solid line) (10^9 molecules cm^{-2} s^{-1}) and the net emission and dry deposition NO_x flux by the big leaf approach, with CRF (squares) and without the CRF (triangles), for a taiga woodland.

lated NO_x fluxes with the big leaf approach without using the CRF, and the biosphere model, both concerning the diurnal cycle and the daily average magnitude. The CRF by YL95 provides a first-order estimate of the NO_x canopy flux divergence for the separate description of the emissions and dry deposition of the big leaf approach. Use of the CRF results in a similar estimate of the NO_x flux divergence for the big leaf and biosphere model for the tropical rain forest whereas the big leaf model calculates a smaller flux divergence for taiga woodland compared to the biosphere model. However, the multilayer vegetation model provides a mechanistic representation of canopy interactions between emissions and dry deposition and is preferred over the big leaf approach, including the CRF, to assess the role of these interactions for the NO_x flux divergence as an explicit function of the involved processes.

5. Discussion

[46] The model comparison of the micrometeorology and atmosphere-biosphere trace gas exchanges has provided important indications about the capability of the 2-layer vegetation and SCM to reproduce the specific micro-meteorological and chemical properties for a tropical and deciduous forest and a taiga woodland. Future research will also focus on the evaluation of the atmosphere-biosphere model for other ecosystems, e.g., savanna and coniferous forest. The selected vertical grid resolution, distinguishing two equidistant layers has been based on a sensitivity study for the tropical rain forest. It has been shown that for this ecosystem the subdivision into a crown layer and a canopy-soil layer is sufficient to resolve the main features of atmosphere-biosphere trace gas exchanges of NO_x and O_3. However, this limited vertical resolution is strongly related to the relevant trace gases, the canopy structure and the degree of detail of the description of the processes involved. JW90 distinguish three layers within the tropical rain forest canopy, the additional third one being a thin layer close to the soil surface. Their vertical grid spacing has been adjusted to resolve the observed vertical gradients of Rn, NO and O_3 and vertical distributions of biomass and stomatal resistances [JW90]. However, this specific information of the vertical distribution of bio-geophysical properties is generally not available for most of the ecosystems represented in large-scale models.

[47] The model evaluation has shown that the representation of the stomatal exchange in the SCM and ECHAM, which largely controls the evapotranspiration and dry deposition fluxes of many gases such as ozone, seems to result in an unrealistic energy partitioning for tropical forest. Moreover, the modeled stomatal exchange is very sensitive to the selected soil moisture, as has been shown in the model evaluation of the modeled micrometeorology over the deciduous forest and taiga canopy. Therefore, future model evaluation should also include the modeled stomatal exchange. We plan to include an alternative representation of the stomatal exchange in the SCM, using a more mechanistic plant-physiological model for CO_2/H_2O exchange [*Ronda et al.*, 2001]. This will allow evaluation of the modeled stomatal exchange, comparing the modeled and observed energy balances as well as the CO_2 fluxes and other trace gas fluxes.

[48] The model evaluation also indicates that the modeled canopy concentrations and canopy top fluxes are sensitive to turbulent transport. In our model, turbulent exchange between the canopy layers and surface layer is calculated using simple "K-theory", and an improved representation should clearly have a high priority for further model development. The turbulent exchange between the canopy and the surface layer determines the residence time of the trace gases in the canopy with its profoundly different biogeochemical environment compared to that of the surface layer. Any improvement in the description of the emissions, dry deposition and chemistry within the canopy is limited by the ability of the model to resolve the atmosphere-biosphere turbulent exchange. Using "K-theory", or first-order closure, to calculate turbulent exchange from the eddy diffusivity and concentration gradient implies that the turbulent exchange is considered to be a down-gradient diffusion process. However, it has been shown that counter-gradient transport occurs regularly, a phenomenon that cannot be reproduced by "K-theory". This occurrence of counter-gradient transport is related to the fact that the turbulent exchange within the canopy is largely controlled by large-scale intermittent down-sweeps, originating in the overlying PBL [*Raupach and Thom*, 1981]. Thus the within canopy turbulent exchange is controlled by nonlocally generated turbulent kinetic energy and, consequently, the local gradient does not necessarily reflect the magnitude and direction of the exchange fluxes. In addition to counter-gradient transfer, the intermittent character of canopy turbulence, associated with the occurrence of a small number of short exchange events that control the average turbulent exchange, is important for atmosphere-biosphere trace gas interactions. Intermittent turbulent exchange may lead to a vertical segregation of reactive trace gases within the canopy and the PBL during quiescent periods. Such periods are followed by bursts into the surface layer of canopy air containing gases from biogenic emissions or chemical production, e.g., NO and NO_2, and mixing into the canopy of trace gases that can subsequently be removed by dry deposition. The penetration depth of the down-sweeps into the canopy and the frequency at which these disturbances occur depend on the turbulent characteristics of the PBL. The intermittent turbulent exchange does not only occur during daytime when convective conditions prevail but also during nighttime. Observations by *Fitzjarrald and Moore* [1990] underscore the role of nocturnal intermittent turbulent exchange for the CO_2, heat and moisture budgets above and within a tropical rain forest canopy.

[49] It is expected that the temporal and spatial average trace gas concentrations and fluxes, considering the intermittent turbulent exchange, are different compared to that for conditions of continuous mixing between the atmosphere and the biosphere. This is caused by the spatial segregation of the reactive species, which reduces the efficiency of second-order chemical reactions, which is expressed by the so-called intensity of segregation (I_s) [*Brodkey*, 1981]. *Patton et al.* [2001] have used a Large Eddy Simulation (LES) model to study the significance of the interactions between turbulence and chemistry within the canopy and surface layer by including multiple scalars that are emitted by the canopy and subjected to varying chemical destruction rates. The scalar source distribution

and chemical destruction rates are selected to mimic the atmosphere-biosphere trace gas exchange of isoprene and the hydroxyl radical (OH). The study indicates that a maximum intensity of segregation of about 17% occurs at the canopy top, which decreases to about 5% at three times the canopy height. Based on the work by *Verver* [1999], *Petersen* [1999] and *Krol et al.* [2000], it is expected that by inclusion of the NO_x chemistry compared to the idealized second-order chemistry considered in the LES model the intensity of segregation for the isoprene-OH system will reduce [*Patton et al.*, 2001].

[50] It is beyond the capability of our model to present the turbulent exchange with the degree of detail compared to models that are specifically developed to study countergradient and intermittent turbulent exchange, such as higher-order closure models [*Meyers and Paw U*, 1987; *Meyers and Baldocchi*, 1991], Lagrangian models [*Raupach*, 1987; *Baldocchi*, 1992] or LES models [*Patton et al.*, 2001]. Rather, parameterizations that account for the nonlocal and intermittent character of the turbulent exchange should be developed from the studies in which these models have been applied.

[51] Besides ignoring the nonlocal and intermittent character of the turbulent exchange, an additional simplification in the representation of turbulent trace gas exchange is that stability effects within the canopy are not considered. The canopy stability often shows a different diurnal cycle compared to the surface layer stability. At night longwave radiative cooling results in a relatively colder canopy top compared to the soil surface, which induces unstable mixing conditions within the canopy. During daytime there is a canopy inversion due to the relatively warmer canopy compared to the soil. Observations of turbulence in a maize crop by *Jacobs et al.* [1992] indicate that during daytime, when large-scale motions control the turbulent exchange, buoyancy effects within the canopy have little or no influence on canopy turbulence. However, the role of the canopy stability becomes relevant for that part of the canopy in which the exchange is not controlled by the large-scale turbulent motions but rather by small-scale diffusion. Observations by *Kruijt et al.* [2000] of the turbulent exchange of CO_2, heat and moisture in a tropical rain forest canopy indicate that especially the lower part of the canopy can be decoupled from the crown layer and the atmosphere. Observed temperature gradients between the crown layer and the soil surface can be as large as 4 K. This thermal stratification suppresses turbulence in the lower part of the canopy since the large-scale turbulent motions are unable to penetrate deeply into the canopy [*Kruijt et al.*, 2000]. During nights with low wind speeds and shear stress, the stability regime expressed by an unstable temperature profile in the canopy controls the nocturnal turbulent exchange, with an inversion layer at the canopy top isolating the canopy interior from the surface layer and PBL. The occurrence of these free convection conditions in the canopy have been observed for different vegetation types [*Jacobs et al.*, 1994; *Bosveld et al.*, 1999]. This is relevant for trace gas exchange in the canopy interior since it increases the efficiency of the nocturnal chemical conversion of gases such as NO and O_3 to NO_2, which can subsequently be removed by dry deposition. It is desirable to include an explicit calculation of the canopy temperature to consider the stability effect within the canopy on turbulent mixing for those conditions for which it is expected that the canopy turbulence is controlled by small-scale motions. Introduction of a canopy temperature is also relevant for other processes. For the calculation of hydrocarbon emissions and chemical transformations within the canopy we have applied the skin temperature of the SCM. This skin temperature reflects the average temperature of the soil and the vegetation. It has been mentioned previously that substantial temperature differences within the canopy can exist, which are significant for hydrocarbon emissions and chemical transformations. Since the hydrocarbon emissions are concentrated in the canopy top due to the optimal conditions in terms of biomass and radiation intensity, the temperature for this reference height should be used.

[52] The model evaluation for the tropical rain forest and deciduous forest sites shows the relevance of changes in surface cover properties due to rainfall and the consequent increase in the wet skin fraction. The surface can also become wet due the formation of dew. Since in our model it is assumed that the dry deposition velocities to wet and dry surfaces are generally different, dependent on the solubility of the trace gas, a sudden increase in the wet skin fraction induces significant changes in the modeled canopy top fluxes. This complicates the model evaluation by comparison with measurements. The uptake or release of trace gases by wet canopies is a process that is not well understood, basically due to the limited number of observations and the complex mechanism that controls the uptake. Several studies have focused on the role of canopy wetness for the ''dry'' deposition of sulfur dioxide indicating that the deposition strongly depends on whether the surface is wetted by rain or dew [*Baldocchi*, 1993, and references therein]. This is related to a different acidity and chemical composition of rain and dew water. This is actually also relevant for other species since the uptake of gases that are not very soluble, e.g., ozone, can be enhanced due to aqueous phase chemistry such as the oxidation of SO_2 by O_3 [*Wesely et al.*, 1990]. Observations of ozone dry deposition fluxes over a deciduous forest by *Fuentes et al.* [1992] show that there is still significant uptake of ozone by a wet canopy due to the formation of dew or rainfall. This is at variance with the assumption of a reduced uptake for wet surfaces made in many deposition models [*Fuentes et al.*, 1992, and references therein], and also in our model. Actually, it can be questioned if there is a reduced uptake by wet vegetation since the leaf stomata are generally at the bottom of the leaves and likely not covered by a water film.

[53] In future, the significance of the uptake by wet foliage will be studied more extensively. Nevertheless, the complexity of the uptake mechanism by wet foliage requires the development of parameterizations that account for this process, which relies on additional measurements of the uptake by wet canopies.

6. Conclusions

[54] We have developed a two-layer vegetation model to describe atmosphere-biosphere trace gas exchanges in large-scale models. The main focus has been the exchange of O_3, NO_x, and NO_y for relative pristine as well as polluted conditions. Our model evaluation indicates that a two-layer

representation of the biosphere can fairly well reproduce the main features of atmosphere-biosphere trace gas exchanges for different canopy structures exposed to different meteorological conditions and trace gas concentrations. The results also indicate that simulations of isoprene emissions require a higher resolution within the crown layer, being well represented by a four-layer model. The results are very sensitive to the selected initial vertical profiles and surface cover properties. By adjustment of the initial vertical profiles and surface properties, the agreement between the modeled and observed meteorology is significantly improved although discrepancies remain, especially concerning the surface energy partitioning. To ensure a realistic representation of the local micrometeorology, future model evaluations could be performed using high-resolution weather prediction models to constrain the SCM.

[55] We generally obtain reasonable agreement between the modeled and observed daytime canopy top ozone fluxes, which suggests that dry deposition and turbulent exchange are realistically described. However, the evaluation of the nocturnal canopy trace gas concentrations and fluxes emphasizes the sensitivity of atmosphere-biosphere trace gas exchange to the nocturnal turbulent exchange. Therefore, future research should address the role of nocturnal free convection conditions within the canopy interior and intermittent exchange for atmosphere-biosphere trace gas exchange. In addition, evaluation of the O_3 deposition fluxes for the tropical rain forest and the deciduous forest has indicated the importance of surface wetness in controlling the dry deposition process.

[56] Unfortunately there are no NO_x flux measurements available for the three sites for which the biosphere model has been evaluated. Consequently, an assessment of the quality of the calculated NO_x canopy fluxes relies heavily on the indirect evaluation through comparison of calculated and observed NO_x concentrations and NO_y canopy fluxes. We generally obtain reasonable agreement between the modeled and observed oxidized nitrogen concentrations and canopy top fluxes. At the deciduous forest and taiga woodland site, the canopy top fluxes of oxidized nitrogen are controlled by the deposition of NO_y due to the significantly larger source of NO_y by advection from source regions compared to the soil biogenic source. Even for a relatively high NO_x to NO_y ratio, the NO_y fluxes are largely controlled by the HNO_3 deposition fluxes due to its large deposition velocity relative to NO_x.

[57] For sites that are exposed to relatively large anthropogenic emission fluxes compared to the soil biogenic emission flux, the big leaf approach and biosphere model calculate similar NO_x fluxes, which confirms the validity of using the big leaf approach for polluted regions. However, for relatively pristine sites such as the tropical rain forest, there are distinct differences between the NO_x canopy top flux of the biosphere model and surface flux by the big leaf approach, both in terms of the diurnal cycle and the daily average absolute magnitude. The canopy reduction factor by YL95 provides a first-order estimate of the reduction of the soil emissions of NO_x due to the canopy interactions. We have compared the applicability of the CRF by comparison of the NO_x fluxes calculated by the big leaf approach, using the CRF and the biosphere model for three ecosystems. Using the CRF does not change the calculated surface flux of NO_x over deciduous forest due to the aforementioned controlling role of advection in the vicinity of anthropogenic emission fluxes. For the tropical rain forest and taiga woodland, where the NO_x concentrations are largely controlled by biogenic emissions, there are significant differences between NO_x fluxes calculated with the big leaf approach and the biosphere model, both concerning the diurnal cycle and the daily average magnitude. However, firm conclusions about the applicability of the CRF on a larger spatial and temporal scale cannot be drawn from this analysis. Therefore, our analysis is extended to a larger selection of ecosystems by performing this comparison on a global scale using the chemistry-GCM ECHAM, presented in an accompanying paper [*Ganzeveld et al.*, 2002].

[58] **Acknowledgments.** This work was performed within the EUSTACH-LBA project (European Studies on Trace gases and Atmospheric Chemistry as a contribution to the Large-scale Biosphere Atmosphere Experiment in Amazonia). We like to thank Erik van Meijgaard from the Royal Netherlands Meteorological Institute (KNMI) for making available the Single-Column Model with ECHAM4-physics and his support with the use of the SCM. We also thank Bert Holtslag and Jordi Vilà-Guerau de Arellano of the Meteorology and Air Quality Group of Wageningen University for their comments. We also would like to thank two anonymous reviewers for their constructive comments. We gratefully acknowledge the supply of observational data of the Harvard Forest site and the Schefferville ABLE-3B site by Bill Munger, Dave Fitzjarrald and Ricardo Sakai.

References

Bakwin, P. S., S. C. Wofsy, S.-M. Fan, M. Keller, S. E. Trumbore, and J. M. Da Costa, Emission of nitric oxide (NO) from tropical forest soils and exchange of NO between the forest canopy and atmospheric boundary layers, *J. Geophys. Res.*, *95*, 16,755–16,764, 1990a.

Bakwin, P. S., S. C. Wofsy, and S.-M. Fan, Measurements of reactive nitrogen oxides (NO_y) within and above a tropical forest canopy in the wet season, *J. Geophys. Res.*, *95*, 16,765–16,772, 1990b.

Bakwin, P. S., et al., Reactive nitrogen oxides and ozone above a taiga woodland, *J. Geophys. Res.*, *99*, 1927–1936, 1994.

Baldocchi, D. D., A lagrangian random-walk model for simulating water vapor, CO_2 and sensible heat flux densities and scalar profiles over and within a Soybean canopy, *Boundary Layer Meteorol.*, *61*, 113–144, 1992.

Baldocchi, D. D., Deposition of gaseous sulfur compounds to vegetation, in *Sulfur Nutrition and Assimilation and Higher Plants*, edited by L. J. De Kok et al., pp. 271–293, SPB Acad. Publ., The Hague, Netherlands, 1993.

Bosveld, F. C., A. A. M. Holtslag, and B. J. J. M. van den Hurk, Nighttime convection in the interior of a dense Douglas Fir forest, *Boundary Layer Meteorol.*, *93*, 171–195, 1999.

Brodkey, R. S., Fundamentals of turbulent motion, mixing and kinetics, *Chem. Eng. Commun.*, *8*, 1–23, 1981.

Cionco, R. M., Analysis of canopy index values for various canopy densities, *Boundary Layer Meteorol.*, *15*, 81–83, 1978.

Deutsches Klimarechenzentrum (DKRZ), The ECHAM3 Atmospheric General Circulation Model, *Modell. Tech Rep. 6*, Hamburg, Germany, 1992.

Duyzer, J., H. Weststrate, and S. Walton, Exchange of ozone and nitrogen oxides between the atmosphere and coniferous forest, *Water Air Soil Pollut.*, *85*, 2065–2070, 1995.

Fan, S.-M., S. C. Wofsy, P. S. Bakwin, D. J. Jacob, and D. R. Fitzjarrald, Atmosphere-biosphere exchange of CO2 and O3 in the Central Amazon forest, *J. Geophys. Res.*, *95*, 16,851–16,864, 1990.

Fitzjarrald, D. R., and D. H. Lenschow, Mean concentration and flux profiles for chemically reactive species in the atmospheric surface layer, *Atmos. Environ.*, *17*, 2117–2120, 1983.

Fitzjarrald, D. R., K. E. Moore, O. M. R. Cabral, J. Scolar, A. O. Manzi, and L. D. De Abreu Sá, Daytime turbulent exchange between the Amazon forest and the atmosphere, *J. Geophys. Res.*, *95*, 16,825–16,838, 1990.

Fitzjarrald, D. R., and K. E. Moore, Mechanism of nocturnal exchange between the rain forest and the atmosphere, *J. Geophys. Res.*, *95*, 16,839–16,850, 1990.

Fitzjarrald, D. R., and K. E. Moore, Growing season boundary layer climate

and surface exchanges in a subartic lichen woodland, *J. Geophys. Res.*, *99*, 1899–1917, 1994.

Fuentes, J. D., T. J. Gillespie, G. den Hartog, and H. H. Neumann, Ozone deposition onto a deciduous forest during dry and wet conditions, *Agric. For. Meteorol.*, *62*, 1–18, 1992.

Galmarini, S., J. Vilà-Guerau de Arellano, and P. G. Duynkerke, Scaling the turbulent transport of chemical compounds in the surface layer under neutral and stratified conditions, *Q. J. R. Meteorol. Soc.*, *123*, 223–242, 1997.

Ganzeveld, L., and J. Lelieveld, Dry deposition parameterization in a chemistry general circulation model and its influence on the distribution of reactive trace gases, *J. Geophys. Res.*, *100*, 20,999–21,012, 1995.

Ganzeveld, L., J. Lelieveld, and G.-J. Roelofs, Dry deposition parameterization of sulfur oxides in a chemistry and general circulation, *J. Geophys. Res.*, *103*, 5679–5694, 1998.

Ganzeveld, L., J. Lelieveld, F. J. Dentener, M. C. Krol, A. F. Bouwman, and G.-J. Roelofs, Global soil-biogenic NOx emissions and the role of canopy processes, *J. Geophys. Res.*, *107*, 10.1029/2001JD001289, in press, 2002.

Gao, W., M. L. Wesely, and I. Y. Lee, A numerical study of the effects of air chemistry on fluxes of NO, NO_2, and O_3 near the surface, *J. Geophys. Res.*, *96*, 18,761–18,769, 1991.

Gao, W., M. L. Wesely, and P. V. Doskey, Numerical modeling of the turbulent diffusion and chemistry of NO_x, O_3, isoprene, and other reactive trace gases in and above a forest canopy, *J. Geophys. Res.*, *98*, 18,339–18,353, 1993.

Guenther, A., et al., A global model of natural volatile organic compound emissions, *J. Geophys. Res.*, *100*, 8873–8892, 1995.

Hicks, B. B., D. D. Baldocchi, T. P. Meyers, R. P. Hosker Jr., and D. R. Matt, A preliminary multiple resistance routine for deriving dry deposition velocities from measured quantities, *Water Air Soil Pollut.*, *36*, 311–330, 1987.

Houweling, S., F. Dentener, and J. Lelieveld, The impact of nonmethane hydrocarbon compounds on troposheric chemistry, *J. Geophys. Res.*, *103*, 10,673–10,696, 1998.

Jacob, D. J., and S. C. Wofsy, Budgets of reactive nitrogen, hydrocarbons and ozone over the Amazon forest during the wet season, *J. Geophys. Res.*, *95*, 16,737–16,754, 1990.

Jacob,, D. J., and P. S. Bakwin, Cycling of NO_x in tropical forest canopies, in *Microbial Production and Consumption of Greenhouse Gases: Methane, Nitrogen Oxides and Halomethanes*, edited by J. E. Rogers and W. B. Whitman, pp. 237–253, Am. Soc. for Microbiol., Washington, D. C., 1991.

Jacobs, A. F. G., J. H. van Boxtel, and R. M. M. El-Kilani, Nighttime free convection characteristics within a plant canopy, *Agric. For. Meteorol.*, *58*, 247–256, 1992.

Jacobs, A. F. G., J. H. van Boxtel, and R. H. Shaw, The dependence of canopy turbulence on within-canopy thermal stratification, *Boundary Layer Meteorol.*, *71*, 375–391, 1994.

Joss, U., and W. K. Graber, Profiles and simulated exchange of H_2O, O_3, NO_2 between the atmosphere and the HartX Scots Pine Plantation, *Theor. Appl. Climatol.*, *53*, 157–172, 1996.

Kramm, G., A numerical method for determining the dry deposition of atmospheric trace gases, *Boundary Layer Meteorol.*, *48*, 157–176, 1989.

Krol, M. C., J. M. Molemaker, and J. Vilà Guerau de Arellano, Effects of turbulence and heterogeneous emissions on photochemically active species in the convective boundary layer, *J. Geophys. Res.*, *105*, 6871–6884, 2000.

Kruijt, B., Y. Malhi, J. Lloyd, A. D. Nobre, A. C. Miranda, M. G. P. Pereira, A. Gulf, and J. Grace, Turbulence statistics above and within two Amazon rain forest canopies, *Boundary Layer Meteorol.*, *94*, 297–331, 2000.

Lelieveld, J., and F. J. Dentener, What controls tropospheric ozone?, *J. Geophys. Res.*, *105*, 3531–3551, 2000.

Meyers, T. P., The sensitivity of modeled SO_2 fluxes and profiles to stomatal and boundary layer resistances, *Water Air Soil Pollut.*, *35*, 261–278, 1987.

Meyers, T. P., and D. D. Baldocchi, The budgets of turbulent kinetic energy and Reynolds stress within and above a deciduous forest, *Agric. Forest. Meteorol.*, *53*, 207–222, 1991.

Meyers, T. P., and K. T. Paw U, Modelling the plant canopy micrometeorology with higher-order closure principles, *Agric. Forest. Meteorol.*, *41*, 143–163, 1987.

Moore, K. E., D. R. Fitzjarrald, R. K. Sakai, M. L. Goulden, J. W. Munger, and S. C. Wofsy, Seasonal variation in radiative and turbulent exchange at a deciduous forest site in central Massachusetts, *J. Appl. Meteorol.*, *35*, 122–134, 1996.

Munger, J. W., S. C. Wofsy, P. S. Bakwin, S.-M. Fan, M. L. Goulden, B. C. Daube, and A. H. Goldstein, Atmospheric deposition of reactive nitrogen oxides and ozone in a temperate deciduous forest and a subartic woodland, 1, Measurements and mechanism, *J. Geophys. Res.*, *101*, 12,639–12,657, 1996.

Norman, J. M., Modeling the complete crop canopy, in *Modification of the Aerial Environment of Crops*, edited by B. J. Barfield and J. F Gerber, pp. 249–280, Am. Soc. of Agric. Eng., St. Joseph, Mich., 1979.

Patton, E. G., K. J. Davis, M. C. Barth, and P. S. Sullivan, Decaying scalars emitted by a forest canopy: A numerical study, *Boundary Layer Meteorol.*, *100*, 91–129, 2001.

Petersen, A. C., Convection and chemistry in the atmospheric boundary layer, Ph.D. thesis, Utrecht Univ., Utrecht, Netherlands, 1999.

Raupach, M. R., A lagrangian analysis of scalar transfer in vegetation canopies, *Q. J. R. Meteorol. Soc.*, *113*, 107–120, 1987.

Raupach, M. R., and A. S. Thom, Turbulence in and above plant canopies, *Ann. Rev. Fluid. Mech.*, *13*, 97–129, 1981.

Raupach, M. R., Simplified expressions for vegetation roughness length and zero-plane displacement as functions of canopy height and area index, *Boundary-Layer Meteorol.*, *71*, 211–216, 1994.

Roberts, J., O. M. R. Cabral, and L. F. De Aguiar, Stomatal and boundary-layer conductance in an Amazonian Terra Firme rain forest, *J. Appl. Ecol.*, *27*, 336–353, 1990.

Roeckner, E., K. Arpe, L. Bengtsson, M. Christoph, M. Claussen, L. Dümenil, M. Esch, M. Giogetta, U. Schlese, and U. Schulzweida, *The Atmospheric General Circulation Model ECHAM-4: Model Description and Simulation of the Present-day Climate*, *Rep. 218*, Max-Planck-Inst. für Meteorol., Hamburg, Germany, 1996.

Roelofs, G.-J., and J. Lelieveld, Distribution and budget of O3 in the troposphere calculated with a chemistry-general circulation model, *J. Geophys. Res.*, *100*, 20,983–20,998, 1995.

Roelofs, G.-J., and J. Lelieveld, Model study of the influence of cross-tropopause O3 transports on tropospheric O3 levels, *Tellus, Ser. B*, *49*, 38–55, 1997.

Roelofs, G.-J., and J. Lelieveld, Tropospheric ozone simulation with a chemistry-general circulation model: Influence of higher hydrocarbon chemistry, *J. Geophys. Res.*, *105*, 22,697–22,712, 2000.

Ronda, R. J., H. A. R. de Bruin, and A. A. M. Holtslag, Representation of the canopy conductance in modeling the surface energy budget for low vegetation, *J. Appl. Meteorol.*, *40*, 1431–1444, 2001.

Sellers, P. J., Y. Mintz, Y. C. Sud, and A. Dalcher, A simple biosphere model (SiB) for use within general circulation models, *J. Atmos. Sci.*, *43*, 505–531, 1986.

Sellers, P. J., W. J. Shuttleworth, J. L. Dorman, A. Dalcher, and J. M. Roberts, Calibrating the Simple Biosphere model for Amazonian tropical forest using field and remote sensing data, I, Average calibration with field data, *J. Appl. Meteorol.*, *28*, 727–759, 1989.

Shuttleworth, W. J., et al., Observations of radiation exchange above and below Amazonian forest, *Q. J. R. Meteorol. Soc.*, *110*, 1163–1169, 1984.

Trumbore, S. E., M. Keller, S. S. Wofsy, and J. M. Da Costa, Measurements of soil and canopy exchange rates in the Amazon rain forest using ^{222}Rn, *J. Geophys. Res.*, *95*, 16,865–16,873, 1990.

Verver, G., Interactions of mixing and chemistry in the atmospheric boundary layer, Ph.D. thesis, Utrecht Univ., Utrecht, Netherlands, 1999.

Vilà-Guerau de Arellano, J., and P. G. Duynkerke, Atmospheric surface layer similarity theory applied to chemically reactive species, *J. Geophys. Res.*, *100*, 1397–1408, 1995.

Walton, S., M. W. Gallagher, and J. H. Duyzer, Use of a detailed model to study the exchange of NO_x and O_3 above and below a deciduous canopy, *Atmos. Environ.*, *31*, 2915–2931, 1997.

Weiss, A., and J. M. Norman, Partitioning solar radiation into direct and diffuse, visible and near-infrared components, *Agric. For. Meteorol.*, *32*, 205–213, 1985.

Wesely, M. L., Parameterization of surface resistances to gaseous dry deposition in regional-scale numerical models, *Atmos. Environ.*, *23*, 1293–1304, 1989.

Wesely, M. L., D. L. Sisteron, and J. D. Jastrow, Observations of the chemical properties of dew on vegetation that affect the dry deposition of SO_2, *J. Geophys. Res.*, *95*, 7501–7514, 1990.

Yienger, J. J., and H. Levy II, Global inventory of soil-biogenic NO_x emissions, *J. Geophys. Res.*, *100*, 11,447–11,464, 1995.

F. J. Dentener, Joint Research Center, Institute for Environment and Sustainability, Ispra I-21020, Italy.

L. N. Ganzeveld and J. Lelieveld, Max-Planck Institute for Chemistry, Joh.-Joachim-Becher-Weg 27, P.O. Box 3060, D-55020 Mainz, Germany.

M. C. Krol and G.-J. Roelofs, Institute for Marine and Atmospheric Research Utrecht (IMAU), Utrecht University, Princetonplein 5, NL-3584 CC Utrecht, Netherlands.